PB 185190

FINAL REPORT

A SURVEY OF METAL OXIDES AS SORBENTS FOR OXIDES OF SULFUR

Contract No. 86-67-51

AVSSD-0043-69-RR

February 1969

Prepared by

AVCO CORPORATION
Space Systems Division
Advanced Chemical Processes Section
Lowell, Massachusetts 01851

Reproduced by the
CLEARINGHOUSE
for Federal Scientific & Technical
Information Springfield Va. 22151

85

FINAL REPORT

A SURVEY OF METAL OXIDES AS SORBENTS FOR OXIDES OF SULFUR

Contract No. 86-67-51

AVSSD-0043-69-RR

February 1969

Prepared by

AVCO CORPORATION
Space Systems Division
Advanced Chemical Processes Section
Lowell, Massachusetts 01851

LIST OF ILLUSTRATIONS

FIGURE 1 TGA Apparatus 15

2 Gas Flow Control. 16

3 Sorption/Regeneration History of Sorbent No. Cu-Al-1. . . 27

4 Porosity Determination of sorbent No. Cu-Al-1 28

5 Sorption/Regeneration History of Sorbent No. Cu-Al-2. . . 31

6 Sorption/Regeneration History of Sorbent No. Al-8A. . . . 32

7 Sorption/Regeneration History of Sorbent No. Al-8B. . . . 33

8 Sorption/Regeneration History of Sorbent No. Cu-Si-1. . . 36

9 Sorption/Regeneration History of Sorbent No. Si-8B. . . . 38

10 Sorption/Regeneration History of Sorbent No. Si-8C. . . . 39

11 Sorption/Regeneration History of Sorbent No. Fe-Al-1. . . 44

12 Sorption/Regeneration History of Sorbent No. Fe-Si-1. . . 46

13 Sorption/Regeneration History of Sorbent No. Mn-Al-2. . . 57

14 Sorption/Regeneration History of Sorbent No. Al-12B . . . 64

15 Sorption/Regeneration History of Sorbent No. Al-12C . . . 65

16 Sorption/Regeneration History of Sorbent No. Al-12D . . . 66

17 Sorption/Regeneration History of Sorbent No. Si-12B . . . 67

18 Sorption/Regeneration History of Sorbent No. Co-Al-1. . . 70

19 Porosity Determination of sorbent No. Fe-Zr-1 73

20 Sorption/Regeneration History of Sorbent No. Fe-Zr-1. . . 74

21 Sorption/Regeneration History of Sorbent No. Ni-Al-1. . . 76

TABLE OF CONTENTS

I. SUMMARY 1

- A. Background 1
- B. Experimental Program 1
- C. Results and Recommendations 1

II. INTRODUCTION 13

- A. General Considerations 13
- B. Sorbent Evaluation 13
  - Determination of Physical and Chemical Properties 13
  - Experimental Procedure 13
  - Procedure for Sorption Rate, Sorption Capacity, and Regenerability 17
  - Weight Gain as an Indication of Sorption 20
- C. Preparation of Sorbents 20

III. SORBENT STUDIES 22

- 1. Copper Oxide-Alumina 22
  - a. Thermochemistry 22
  - b. Preparation and Evaluation 24
- 2. Copper Oxide-Silica 34
  - a. Thermochemistry 34
  - b. Preparation and Evaluation 35
- 3. Iron Oxide-Alumina 40
  - a. Thermochemistry 40
  - b. Preparation and Evaluation 40
- 4. Iron Oxide-Silica 43
  - a. Thermochemistry 43
  - b. Preparation and Evaluation 45
- 5. Manganese Oxide-Alumina 45
  - a. Thermochemistry 45
    - One-Stage Regeneration with Reducing Gas 49
    - Two-Stage Regeneration with Reducing Gas 53
  - b. Preparation and Evaluation - Manganese Oxide-Alumina 55

APPENDIX I 58

Summary of Sorbents Exhibiting Marginal Performance 58

TABLE OF CONTENTS (cont'd)

1. Co-Precipitated Sorbents 58

   a. Series I, Al-1 through Al-14 58

   b. Series II, Al-8A, B, C; Si-8A, B, C,; Al-9A, B, C; Al-12B, C, D; Si-12B, C, D. 58

   c. Series III - Cu-V-1, 2; Co-Al-1; Cr-Al-2; Fe-V-1; Fe-Zr-1; Mn-Si-1; Mn-V-1; Ni-Al-1. 68

2. Sorbents Made by Impregnation. 75

3. Commercially Available Sorbents. 78

APPENDIX II. 79

LIST OF TABLES

TABLE I Sorption and Regeneration Characteristics. 4

II Sorbents Arranged According to Capacity. 8

III Sorbents Arranged According to Percent Utilization of Stoichiometric Capacity 10

IV Sorbents Arranged According to Initial Rate. 11

V Sorbents Arranged According to Half-Time 12

VI Precipitation Ranges in NH_4OH and $(NH_4)_2CO_3$. 21

VII Equilibrium Product Distribution for SO_2 Sorption on Copper Oxide 23

VIII Equilibrium Product Distribution for Regeneration of Cu_2SO_5 in Oxygen-Nitrogen Gas. 25

IX Equilibrium Product Distribution for Sorption of SO_2 on Excess Iron Oxide. 41

X Equilibrium Product Distribution for Thermal Regeneration of Ferric Sulfate in Nitrogen. 42

XI Sorption of Flue Gas on Mn_2O_3. 48

XII $MnSO_4$ Regeneration in Nitrogen 50

XIII Summary of Equilibrium Computations on One-Stage Regeneration 52

XIV Properties of Co-Precipitates, Series I. 59

XV Properties of Co-Precipitates, Series II 63

XVI Properties of Impregnates Sorbents 77

BLANK PAGE

I. SUMMARY

A. Background

Alkalized alumina has for some time been under consideration as a sorbent for the removal of sulfur oxides from flue gas. It has the ability to significantly reduce the level of sulfur oxides concentration in a flue gas and is capable of subsequent regeneration in a reducing atmosphere. Some inadequacies have been encountered with alkalized alumina, however. Most significant of these is the poor physical strength of the particles which causes large attrition losses in use. In addition, the requirement of different temperatures for sorption and regeneration steps, nominally 350 and 650°C, respectively, places a burden of additional heat exchange on the process. The requirement for chemical regeneration (e.g., hydrogen) also contributes to the cost of the process. Finally, although sorption and regeneration rates on alkalized alumina appear to be satisfactory, any improvement of rate could only be considered advantageous. The desirability of an alternative solid sorbent to overcome these weaknesses is apparent. This study was thus undertaken to assess the possibility of utilizing one of several possible chemically active metal oxides to sorb oxides of sulfur from flue gas.

B. Experimental Program

In the course of this study seventeen metal oxides, on one or more supporting oxides, were evaluated for their sorbing and regenerating characteristics. The sorbents investigated were for the most part made by co-precipitation of the hydroxides of the "active" and "supporting" oxides followed by calcining, analogous to the preparation of alkalized alumina. Several catalyst supports impregnated with the "active oxide" as well as commercially available materials were also evaluated.

The extent and rate of sorption and regeneration of these materials was determined by following the weight change of a sample exposed to a synthesized typical flue or regenerating gas with time (see page 17). A thermal gravimetric analysis (TGA) apparatus, consisting of an analytical balance supporting a basket of the sample in a furnace tube with the flue gas atmosphere (see page 14) was used for these evaluations. Regeneration of sulfur-loaded sorbents was carried out thermally (in nitrogen) or chemically (in hydrogen).

Where thermochemical data could be found, equilibrium for sorption of sulfur oxides was calculated and compared to actual experimental results. These computations were frequently very helpful in predicting or explaining the behavior of some sorbents.

C. Results and Recommendations

The best overall perspective of this survey may be gained from Table I (pages 4-7) in which every sorbent evaluated is presented. The arrangement of this table is alphabetic according to the chemical symbol of the cationic portion of first the "active oxide" and then the "supporting oxide". The next columns indicate the weight percent of "active oxide" (page 13), the stoichiometric capacity (page 13) and the surface area (page 13) of the sorbent. The central portion of the table gives a summary of the sorption characteristics of a given sorbent at $300^{\circ}C$, $450^{\circ}C$, and $550^{\circ}C$. Since the purpose of this table is to summarize the performance of all the sorbents investigated in this study, the values given for any set of conditions are the average of the results which are presented in much greater detail in the body of the report. The sorption characteristics listed are defined as follows: The initial rate is the sorption rate at time = 0, where the rate is grams of SO_2/100 grams sorbent - hour - mole fraction SO_2 in the flue gas; the percent utilization of stoichiometric capacity (page 13) is an indication of the extent of reaction of SO_2 with the amount of "active oxide" in the sorbent as found by analysis (page 13); the half times for a sorption and subsequent regeneration are the time required to sorb to one half of saturation for the particular sorbent under the condition indicated (page 19).

A comparison of the relative performance of each of the materials evaluated is given in Tables II, (page 8) III, (page 10) IV, (page 11) and V (page 12). These tables list each sorbent according to stoichiometric capacity, percent utilization, initial rate, and half-time, with the sorbent showing the best value being placed at the top of the list.

On comparing these four tables one finds that some of the copper oxide-alumina and manganese oxide-alumina sorbents, namely: Cu-Al-1, Au-Al-2, Mn-Al-2, and Al-9A occur in high positions in Tables III, IV, and V. This reflects the generally good performances of these sorbents. Other sorbents occupy a combination of both high and low positions in these tables.

Sorbents with higher stoichiometric capacities, a quality which is directly related to the amount of active oxide in the sorbent, were found to have lower surface areas reflecting a less porous structure. Porosity is the most important single factor on the extent of utilization of the stoichiometric capacity of a given sorbent. Thus, the higher the stoichiometric capacity, the less accessible is that capacity. For this reason, sorbents with high percent utilization are generally very low on the stoichiometric capacity list. Again, a higher proportion of active oxide in the sorbent reduces the porosity.

Tables IV (page 11), and V (page 12) which are listed according to initial rate and half-time, respectively, are two different aspects of the same phenomenon, namely, sorption rate. One would therefore expect fast acting sorbents to appear in high positions in both these lists. This is certainly true for Cu-Al-1 and Cu-Al-2. That there is not a better correspondence for more sorbents in these two lists is a result of other factors. A high initial rate can decline very rapidly and if the sorption then continues for a long time at a slower rate, the high initial rate has little influence on the half-time which will then become large, as was the case with Mn-Al-2. On the other hand, a sorption which has a moderate initial rate but sustains a good rate throughout the sorption can have a relatively good half-time, such as Al-9-A, Al-12-D, and Al-12B. It is interesting to note that both the copper oxide-alumina sorbents, Cu-Al-1, Cu-Al-2, share high initial rates as well as short half-times, indicating a sustained high sorption rate.

As was mentioned earlier, a sorbent with a higher proportion of active oxide generally has a lower porosity. Low porosity would be expected to result in low sorption rate, both initially and throughout the sorption. From this it follows that sorbents with high stoichiometric capacity (resulting from high proportion of active oxide - hence low porosity) would not show good sorption rates. This is unequivocally demonstrated in Tables IV and V.

All of the sorbents prepared and evaluated in this study were found to be thermally regenerable at a temperature of about 650°C. In this regard, they have an advantage over alkalized alumina which requires a reducing atmosphere. Thermal regeneration may not be practical, however, where the concentration of sulfur compounds in the regenerate gas is low. Hydrogen regeneration was also attempted with one of the copper oxide-alumina sorbents (Cu-Al-2). With this sorbent, it was determined that complete regeneration was realized at 400°C to 450°C, a temperature at which sorption of SO_2 also proceeds very satisfactorily. This suggests the possibility of a sorption-regeneration cycle all at the same temperature and obviates the cost of heat exchange required by the differing sorption and regeneration temperatures necessary with alkalized alumina.

The outstanding performance of the copper oxide sorbents in this study suggests that further investigation of this material should be undertaken. Manganese and iron oxide sorbents showed promising rates and capacities and might well merit further work.

TABLE I

SORPTION AND REGENERATION CHARACTERISTICS

Active Oxide	Supporting Oxide	Wt. % Active Oxide	Stoich. Cap. gm SO_2/100 gm sorb.	Surface Area, $\frac{m^2}{gm}$		300°C				450°C				550°C				Sorbent Designation	Page Number	Remarks
						Initial Rate mg SO_2/% SO_2 hr.	% Stoich. Cap.	Half time, min.	Nominal Regen. Half time, min.	Initial Rate mg SO_2/% SO_2 hr.	% Stoich. Cap.	Half time, min.	Nominal Regen. Half time, min.	Initial Rate mg SO_2/% SO_2 hr.	% Stoich. Cap.	Half time , min.	Nominal Regen. Half time , min.			
Cu	Al	37.7	30	242		204	49	3	7	222	56.5	14.5	17.5	198	75	18	26.5	Cu-Al-1	24	
		28.9	23.2	184		295	141	6.5	5	384	152	8.7	5	550	142	10	5	Cu-Al-2	29	H_2 Regen.
		11.6	9.03	224		197	157	29	10	166	176	58	12	28	20	3	7	Al-8-A	30	
		34.4	27.4	74		76.6	34	25		22	15.3	45		-	-	-		Al-8-B	30	
		75.3	62	10.5			1				6					5		Al 8-C	30	
	Al	16.8	15	175-220			40				49					-		Al-8	58	
		10	13	137														-	78	Harshaw $CuO-Al_2O_3$
	Al-Si	-	-	-														I-6	75	
Cu	Si	59	97	48		234	11	57	14	557	72	40.5	60	400	73	17	140	Cu-Si-1	35	
		4.75	3.8	3.0		-	0	-	-	-	0	-	-	-	0	-	-	Si-8A	37	
		14.4	12	102		43	83	24	9	30	61.5	2.75	10	185	23	1.3	-	Si-8B	37	
		43.5	36	4.5		15.5	21.5	59	18	130	48.5	20.5	38	170	18	9	25	Si-8C	37	

TABLE I (Cont'd)

SORPTION AND REGENERATION CHARACTERISTICS

Active Oxide	Supporting Oxide	Wt. % Active Oxide	Stoich. Cap. gm SO_2/100 gm sorb.	Surface Area, $\frac{m^2}{gm}$		300°C				450°C				500°C				Sorbent Designation	Page Number	Remarks
						Initial Rate mg SO_2/% SO_2 hr.	% Stoich. Cap.	Half time, min.	Nominal Regen. Half time, min.	Initial Rate mg SO_2/% SO_2 hr.	% Stoich. Cap.	Half time, min.	Nominal Regen. Half time, min.	Initial Rate mg SO_2/% SO_2 hr.	% Stoich. Cap.	Half time, min.	Nominal Regen. Half time, min.			
Cu	V	-	-	0		-	-	-	-	-	-	-	-	-	-	-	-	Cu-V-1	68	Unsatisfactory
Co	Al	49	125	171		90	4	13	19	125	5	5	8	-	-	-	-	Co-Al-1	69	
Cr	Al	52.2	65	-		-	-	-	-	-	-	-	-	-	-	-	-	Cr-Al-2	69	
		-	-	131														Al-6	58	
Cr	Al-Si	2.4	3.0	24.4														I-4	75	
Fe	Al	46	55	233		85	40	121	8	65	8	11	8	-	-	-	-	Fe-Al-1	40	
		4.70	5.65	376		15	30.5	4	14	53	41	7	21	-	16	6	-	Al-12-B	62	
		13.6	16.3	340		38	33	10	23	23	37	19.5	65	0	0	60		Al-12C	62	
		33.4	40.1	274		26	2	3		54	3	4		31	0.1	3		Al-12D	62	
		54.2	73	146														Al-12	58	
	Al-Si	9.2	11.3	-			0.03				0.25							I-8	75	
	Al-Si	3	3.7																78	Fluorite

TABLE I (Cont'd)

SORPTION AND REGENERATION CHARACTERISTICS

Active Oxide	Supporting Oxide	Wt. % Active Oxide	Stoich. Cap. gm SO_2/100 gm sorb.	Surface Area, $\frac{m^2}{gm}$		300°C				450°C				550°C				Sorbent Designation	Page Number	Remarks
						Initial Rate mg SO_2/% SO_2 hr.	% Stoich. Cap.	Half time, min.	Nominal Regen. Half time, min.	Initial Rate mg SO_2/% SO_2 hr.	% Stoich. Cap.	Half time, min.	Nominal Regen. Half time, min.	Initial Rate mg SO_2/% SO_2 hr.	% Stoich. Cap.	Half time, min.	Nominal Regen. Half time, min.			
Fe	Si	42.5	48	248		0	0	-	-	50	40	120	30	24	6.5	21	11	Fe-Si-1	45	
		4.35	4.22	163		0	0	-	-	31	26	11	8	31	32	5	2	Si-12B	62	
		10.8	13	258		0	0	-	-	30	31	12	3	71	10	4	3	Si-12C	62	
		26.8	32	174		0	0	-	-	25	5	8	3	10	1	14	3	Si-12D	62	
Fe	V	53	60	1.1		-	0	-	-	0	-	-	-	-	0	-	-	Fe-V-1	71	
Fe	Zr	33.6	40	272		10	22	105	8	129	16	14	3	61	6	4	8	Fe-Zr-1	71	
K	Al	16.7	17	32		-	21	5										Al-3	58	
	Al-Si	-	-	6.8			-				-				-			I-1	75	
Li	Al	14.8	32	135														Al-1	58	
		13.3	31	9.6			8				10							Al-2	58	
Mn	Al	37.8	34	198		400	30	13	-	400	33	11	5	280	39	10	5	Mn-Al-2	55	
		98	110	-														Al-9	58	
		1.55	1.4	304		61	146	4	18	46	110	5	26	66	118	4	18	Al-9-A	62	
		1.91	1.72	306		38	77	5	15	9	74	15	14	57	85	4	25	Al-9-B	62	

TABLE I (Concl'd)

SORPTION AND REGENERATION CHARACTERISTICS

Active Oxide	Supporting Oxide	Wt. % Active Oxide	Stoich. Cap. gm SO2/100 gm sorb.	Surface Area, $\frac{m^2}{gm}$		300°C				450°C				550°C				Sorbent Designation	Page Number	Remarks
						Initial Rate mg SO_2/% SO_2 hr.	% Stoich. Cap.	Half time, min.	Nominal Regen. Half time, min.	Initial Rate mg SO_2/% SO_2 hr.	% Stoich. Cap.	Half time, min.	Nominal Regen. Half time, min.	Initial Rate mg SO_2/% SO_2 hr.	% Stoich. Cap.	Half time, min.	Nominal Regen. Half time, min.			
		2.86	2.59	289		42	69	8	18	37	29	4	24	3	17	8	20	Al-9C	62	
	Al-Si	7.3	6.6	245														I-7	75	
Mn	Si	39	35	36		-	0	-	-	-	0	-	-	-	38	50	00	Mn-Si-1	72	
Mn	V	62	56	1.1		-	1	10	15	-	7	40	5	-	3	-		Mn-V-1	72	
Na	Al	8.6	9.4	152														Al-4	58	
Na	Al-Mn																	Al-14	58	
Na	Al-Si	-	-	20														I-2	75	
Ni	Al	26.4	23	306		189	19	15	1	221	11	12	1	106	12	6	1	Ni-Al-1	75	H_2 Regen.
		24.7	23	275			-				-				-			Al-5	58	
	Al-Si	-	-	24														I-3	75	
Zn	Al	17.0	15	175														Al-7	58	
	Al-Si	-	-	22.8														I-5	75	
-	-	-	-	-		-	-	-	-	-	-	-	-	-	-	-	-	-	78	Linde Mol Sieve 5A

Table II

Sorbents Arranged According to Stoichiometric Capacity

Designation	Stoichiometric Capacity (gm SO_2/ 100 gm Sorbent)	% Utilization of Stoichiometric Capacity Realized at 300°C	Initial Rate at 300°C (gm SO_2/100 gm Sorbent-hr.-mol fract. SO_2)	Half-Time at 300°C (min.)
Co-Al-1	125	4	90	13
Al-9	110	-	-	-
Cu-Si-1	97	11	234	57
Al-12	73	-	-	-
Cr-Al-2	65	-	-	-
Al-8-C	62	1	-	-
Fe-V-1	60	0	-	-
Mn-V-1	56	1	-	10
Fe-Al-1	55	40	85	121
Fe-Si-1	48	0	0	-
Al-12-D	40	2	26	3
Fe-Zr-1	40	22	10	105
Si-8-C	36	22	15	59
Mn-Si-1	35	0	-	-
Mn-Al-2	34	30	400	13
Si-12-D	32	0	0	-
Al-1	32	-	-	-
Al-2	31	8	-	-
Cu-Al-1	30	49	204	3
Al-8-B	27	34	77	25
Cu-Al-2	23	141	295	7
Ni-Al-1	23	19	189	15
Al-5	23	-	-	-
Al-12-C	16	33	38	10
Al-8	15	40	-	-
Al-7	15	-	-	-
Harshaw $CuO-Al_2O_3$	13	1	-	-
Si-12-C	13	0	0	-
Si-8-B	12	83	53	24
Al-3	12	21	-	5
I-8	11	0.03	-	-

Table II continued

Designation	Stoichiometric Capacity (gm SO_2/ 100 gm Sorbent)	% Utilization of Stoichiometric Capacity Realized at 300°C	Initial Rate at 300°C (gm SO_2/100 gm Sorbent-hr.-mol fract. SO_2)	Half-Time at 300°C (min.)
Al-4	9	-	-	-
Al-8-A	9	157	197	29
I-7	7	-	-	-
Al-12-B	6	30	15	4
Si-12-B	5	0	0	-
Si-8A	4	0	-	-
Florite	4	-	-	-
I-4	3	-	-	-
Al-9-C	3	69	42	8
Al-9-B	2	77	38	5
Al-9-A	1	146	61	4

Table III

Sorbents Arranged According to Percent Utilization of Stoichiometric Capacity

Designation	% Utilization of Stoichiometric Capacity Realized at 300°C	Stoichiometric Capacity (gm SO_2/ 100 gm Sorbent)	Initial rate at 300°C (gm SO_2/100 gm Sorbent-hr.-mol fract. SO_2)	Half-time at 300°C (min.)
Al-8A	157	9	197	29
Al-9-A	146	1	61	4
Cu-Al-2	141	23	295	7
Si-8-B	83	12	53	24
Al-12-C	77	16	38	10
Al-9-C	69	3	42	8
Cu-Al-1	49	30	204	3
Fe-Al-1	40	55	85	121
Al-8-B	34	27	77	25
Al-9-B	33	2	38	5
Al-12-B	31	6	15	4
Mn-Al-2	30	34	400	13
Fe-Zr-1	22	40	10	105
Si-8-C	22	36	15	59
Cu-Si-1	11	97	234	57
Co-Al-1	4	125	90	13
Al-12-D	2	40	26	3

Table IV

Sorbents Arranged According to Initial Rate

Designation	Initial Rate at 300°C ($gm\ SO_2/gm$ Sorbent-hr.-mol fract. SO_2)	Half-Time at 300°C (min.)	Stoichiometric Capacity ($gm\ SO_2$/100 gm Sorbent)	% Utilization of Stoichiometric Capacity Realized at 300°C
Mn-Al-2	400	13	34	30
Cu-Al-2	295	7	23	141
Cu-Si-1	234	57	97	11
Cu-Al-1	204	3	30	49
Al-8A	197	29	9	157
Ni-Al-1	189	15	23	19
Co-Al-1	90	13	125	4
Fe-Al-1	85	121	55	40
Al-8-B	77	25	27	34
Al-9-A	61	4	1	146
Si-8B	53	24	12	83
Al-9-C	42	8	3	69
Al-12-C	38	10	16	77
Al-9-B	38	5	2	33
Al-12D	26	3	40	2
Si-8C	16	59	36	22
Al-12-B	15	4	6	31
Fe-Zr-1	10	105	40	22

Table V

Sorbents Arranged According to Half-Time

Designation	Half-Time at 300°C (min.)	% Utilization of Stoichiometric Capacity Realized at 300°C	Initial Rate at 300°C (gm SO_2/100 gm Sorbent-hr.-mol fract. SO_2)	Stoichiometric Capacity (gm SO_2/ 100 gm Sorbent)
Cu-Al-1	3	49	204	30
Al-12-D	3	2	26	40
Al-9-A	4	146	61	1
Al-12-B	4	31	15	6
Al-9-B	5	33	38	2
Cu-Al-2	7	141	295	23
Al-9-C	8	69	42	3
Al-12-C	10	33	38	16
Mn-Al-2	13	30	400	34
Co-Al-1	13	4	90	125
Ni-Al-1	15	19	189	23
Si-8-B	24	83	53	12
Al-8-B	25	34	77	27
Al-8-11	29	157	197	9
Cu-Si-1	57	11	234	97
Si-8C	59	22	16	36
Fe-Zr-1	105	22	10	40
Fe-Al-1	121	40	85	55

II. INTRODUCTION

A. General Considerations

The ability of a material to sorb sulfur oxides depends to a large extent on the chemistry of the sorbent and sorbate; metal oxide and sulfur oxides in this case. Chemical equilibrium must, of course, be favorable for both the sorption and desorption (regeneration) if the system is to be successful, since it is equilibrium which sets the limits on the extent to which a flue gas can be cleaned of sulfur oxides and the nature and concentration of sulfur compounds in the regenerate gas.

Of equal importance is the rate at which these sorption and desorption reactions occur since it strongly influences the economics of the process. The sorption process may be considered as the sequence in which sulfur oxide is carried in the flue gas stream to the outside of the sorbent material where it finds its way to the sorption sites by diffusion through the pores of the sorbent. Having reached such a site, the actual bonding reaction between sulfur oxide and sorbent takes place. Each of these steps has a characteristic rate. If any one step in the sequence is significantly slower than the other, the rate for the total processes will be that of the slow step. Thus, the rate limiting step could be bulk mass transfer or pore diffusion or sorbent-sorbate reaction rate, for example. In some cases in the discussion of results of this study it was possible to determine which mechanism was the rate limiting step, by correlating with appropriate mathematical models.

B. Sorbent Evaluation

Determination of Physical and Chemical Properties

1. Surface Area

The surface area of each sorbent was determined by the BET method using adsorption of nitrogen in a Perkins-Elmer 212 C Sorptometer.

2. Active Oxide Content

Each sorbent was analyzed, using standard wet chemical techniques, to determine the amount of active oxide, supporting oxide or both. In cases where only one constituent was determined, the other was taken as the difference, allowing for volatiles. Since these quantitative analyses could only be made for the metal and not the oxide, the results have been reported as the metal corresponding to the specified amount of oxide. The question of which oxide, in cases where several were possible such as iron and manganese, was resolved by x-ray analysis or thermodynamics.

3. Stoichiometric Capacity

Having determined the amount and type of active oxide present in a sorbent, the capacity for sulfur oxides, based on a reaction between the active oxide present and sulfur trioxide, was computed. The stoichiometric capacity considers the reaction of all the active oxides and is expressed in terms of sulfur dioxide.

Experimental Procedure

1. TGA Apparatus

The sorption and regeneration data are obtained by measuring changes in the weight of a sample of sorbent during exposure to simulated flue and regeneration gases. The weight is determined in a TGA type apparatus.

The apparatus consists of a means of supporting and weighing a sample of sorbent which is held at constant temperature in a controllable atmosphere. The support and weighing system, the temperature control, and the gas supply system will be described in turn. Standard operating conditions will then be given.

2. Support and Weighing System

The sample of sorbent is supported in a basket suspended from a Mettler, H-6T balance. The balance is used to determine the sample weight to an accuracy of ± 0.2 mg. The sample basket is surrounded by a quartz tube with an I.D. of 1.5 inches. Gases enter from the bottom of the tube. A two zone furnace surrounds the tube. This equipment is shown schematically in Figure 1.

A light chain is used to connect the sample basket to the balance. A loop and hook attached to the chain allow positioning of the sample in the center of the hot zone or the cold zone without opening the apparatus.

3. Temperature Control

A Lindburgh Hevi-Duty furnace, Model M-1018-S surrounds the quartz tube. There are two zones in the furnace and the temperature of each is controlled with an API Model 712 controller. The temperature is sensed with chromel-alumel thermocouples. The bottom of the quartz tube is packed with glass beads for uniform distribution and gas preheat.

The sample is supported in the cold zone (300°C) for sorption and is moved to the hot zone (650°C) for regeneration by shortening the support chain.

4. Gas Flow Control

A schematic of the gas flow control system is shown in Figure 2. Valves S-1 and S-2 are three-way solenoids that are simultaneously operated by a single switch. In the purge position, S-1 allows purge N_2 to enter the TGA while the simulated flue gas or H_2 entering S-2 is diverted to the hood. The alternate position closes off the by-pass and purge N_2 lines and allows the flue gas or H_2 to flow through S-2 and S-1 to the TGA.

To effect a sorption or regeneration, the sorbent is exposed to flue gas or nitrogen, respectively, for a short period of time. At the end of the desired interval the solenoids are put in the purge position for 10 seconds, thus sweeping all reactive gases from the TGA. The purge N_2 is then shut off and the sample weight taken in static N_2. The solenoids are then switched to the alternate position allowing a second interval of sorption or regeneration to begin. Data are generated as tables of weight gain or loss vs. time. The transitory sorptions were necessary because "noise" on the balances was caused by slight variations in flow around the particles and hence, the weight could not be determined with the flue gas flowing through the tube.

FIGURE 1 TGA Apparatus

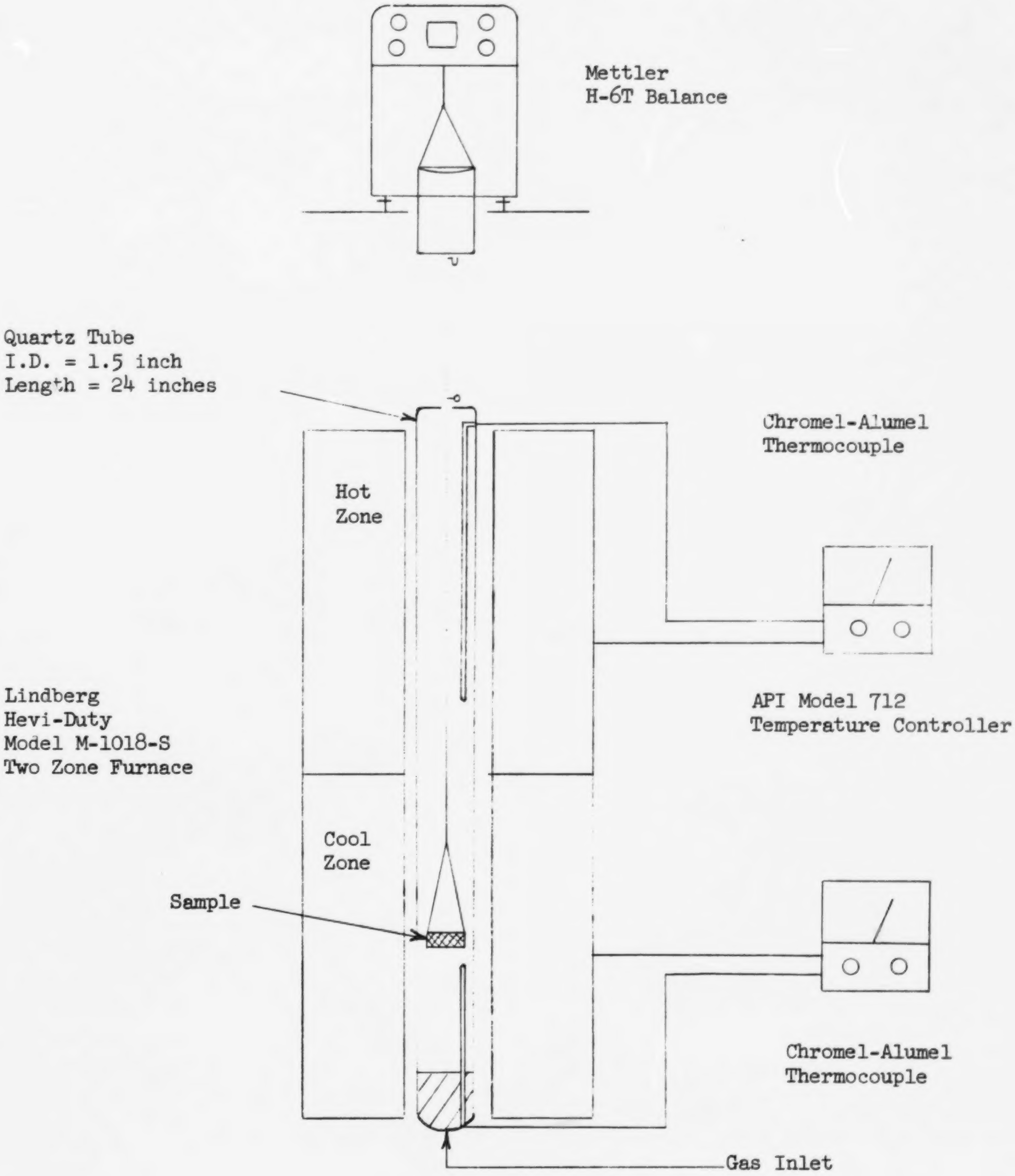
Mettler
H-6T Balance
Quartz Tube
I.D. = 1.5 inch
Length = 24 inches
Chromel-Alumel
Thermocouple
Hot
Zone
Lindberg
Hevi-Duty
Model M-1018-S
Two Zone Furnace
API Model 712
Temperature Controller
Cool
Zone
Sample
Chromel-Alumel
Thermocouple
Gas Inlet

FIGURE 2 Gas Flow Control

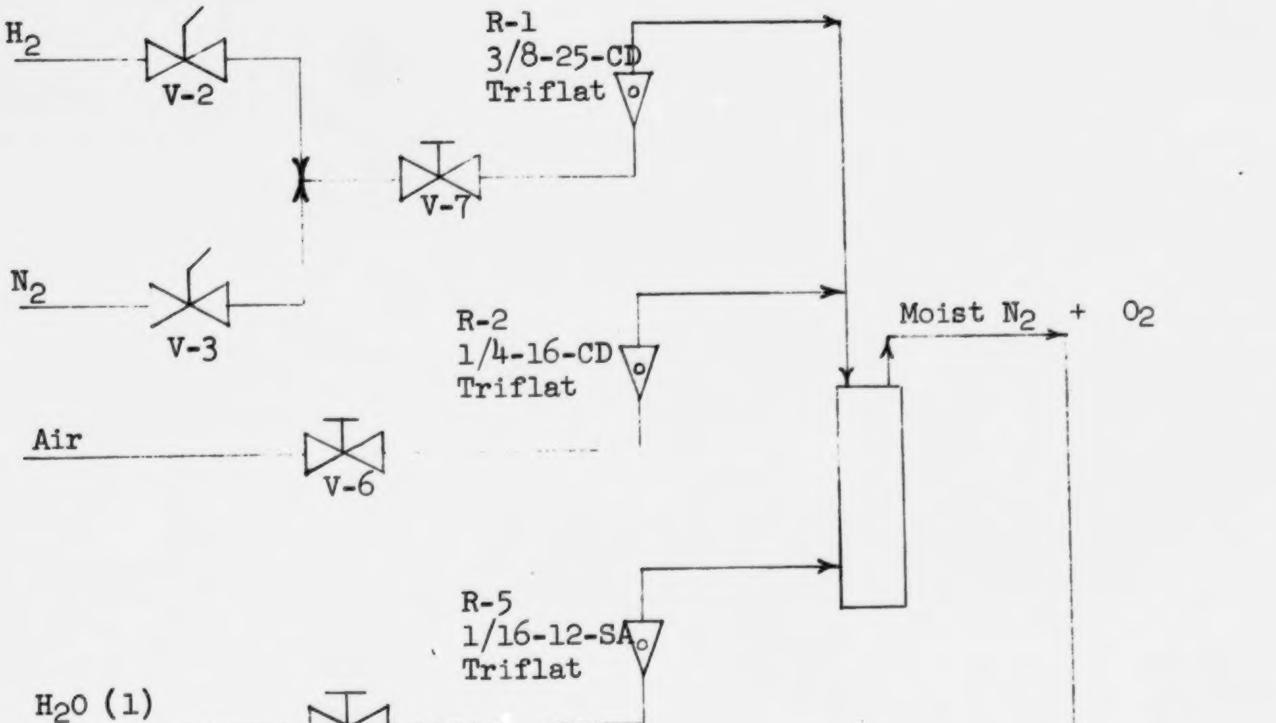
H_2
V-2
N_2
V-3
V-7
R-1
3/8-25-CD
Triflat
R-2
1/4-16-CD
Triflat
Moist N_2 + O_2
Air
V-6
R-5
1/16-12-SA
Triflat
H_2O (1)
V-9
R-3
1/16-08-SA
Triflat
V-5
NO
R-4
1/16-08-SA
Triflat
V-8
SO_2
S-2
Bypass
R-6
1/4-20-CD
Purgerater
S-1
To TGA
Purge N_2
V-1
V-4

The simulated flue gas for sorption consists of N_2, O_2, H_2O, NO_x, and SO_2. CO_2 was not included in the simulated flue gas as it was determined in early experiments that the sorption of CO_2 on alkalized alumina was negligibly slow. The proper N_2/O_2 mixture is obtained by metering dry air and N_2 through rotameters R-2 and R-1, respectively. This mixture is then led to a vaporizer to which liquid water is metered through rotameter R-5. All lines subsequent to the vaporizer are traced with heating tapes. NO_x and SO_2 are added to the moist N_2/O_2 mixture downstream of the vaporizer. Flows of these gases are also metered with rotameters.

5. Conditions of Operation

Sorption temperature:	300°C, 450°C, 550°C
Sorption pressure:	1 atm
Simulated flue gas:	

Component	Mole Fraction
N_2	0.894
O_2	0.029
H_2O	0.075
NO_x	0.0005
SO_2	0.00324

Superficial gas velocity during sorption:	2.4 ft/sec
Total simulated flue gas flow:	24.3 SLPM
Regeneration temperature:	650°C
Regeneration gas:	H_2
Regeneration gas flow:	10.4 SLPM
Superficial gas velocity during regeneration:	47.3 cm/sec, 1.55 ft/sec

Procedure for Sorption Rate, Sorption Capacity, and Regenerability

1. Step by step procedure

   a. Fresh sorbent is packed in a tube furnace and activated in N_2 at 650°C for 4 hours. The superficial velocity is 12 cm/sec.

   b. A sample of activated sorbent weighing approximately 500 mg is charged to the TGA apparatus.

   c. The sample is exposed to an SO_2 free simulated flue gas of the following composition:

N_2 - 89.4% by volume

O_2 - 2.9%

H_2O - 7.5%

NO_x - 500 ppm

d. When the sample is equilibrated with the SO_2 free flue gas the sorption cycle is begun. Flue gas identical to that shown above with the addition of 0.324% by volume SO_2 is used. Initial sorption intervals between weighings are 15 seconds. Near saturation, where the rate of sorption is much slower, intervals of 10 to 30 minutes are used.

e. When no further weight gain is observed, the sorption is complete and the sorbent is saturated. From the weight gains and time intervals a table of weight gain vs. time can be constructed.

f. The regeneration is then started by raising the sorbent basket to the 650°C zone and changing to nitrogen in the TGA.

g. After one minute, the flow of nitrogen is stopped and the weight loss determined.

h. Step g is repeated at intervals expanding to several minutes at the completion of regeneration. This generates the data for a table of weight loss vs. time exactly analogous to the sorption data.

i. Steps c through h are repeated to give as many sorption regeneration cycles as desired.

2. Basic Sorption Series

To evaluate each sorbent, a basic sequence was devised and used throughout the study. This consisted of six sorption-regeneration cycles. The first two sorptions were at 300°C, followed by two at 450°C, and finally two at 550°C. Regeneration was at 650°C.

Deviations from this sequence are noted where applicable.

3. Data Reduction and Presentation

a. Sorption data

The sorption data are presented as sorption capacity in weight SO_2/100 weights of sorbent and as normalized sorption rate vs. loading.

The normalized sorption rate is derived from an assumed sorption rate expression of the form

$$dW/dt = y \cdot f(W)$$

where W = sorbent loading, gm SO_2/gm sorbent

y = mole fraction SO_2 in gas

t = time

f = function of W

The normalized sorption rate is

$$(1/y)\,(dW/dt)$$

and is given units of hr^{-1}, and when plotted vs. W the resulting curve is f(W).

Values of the normalized sorption rate are determined by numerically differentiating the weight gain vs. time curves using three-point Lagrangian differentiation formulas.

The half-times for a sorption and subsequent regeneration are the times at which the weight gain corresponds to one half the saturation weight gain. These half times are presented only to make possible a comparison of the numerous sorbents evaluated in this study and hence should not be construed as an indication that these sorptions are strictly first order processes.

b. Sorption-Regeneration History Charts

This type figure was devised to present the salient features of the "basic" sorption series for each sorbent. The description of Figure 3 (page 27) for Cu-Al-1 is thus generally applicable to the equivalent figure for other sorbents. Most of the numerical values given in the table are self-explanatory or have been explained elsewhere in this report; however, several remarks are in order. The designations S1, R1, S2, R2, etc., correspond to first sorption, first regeneration, second sorption, second regeneration, i.e., the actual sequence of the series. The loading vs. time curve takes as zero loading the weight of the sample after it has been brought to temperature in the simulated flue gas - less SO_2. The time units of the absisca are arbitrary, but the general shape of the sorption-time curve is preserved. It will be noted that regeneration to constant weight, does not always coincide with the base line. The difference corresponds to a net gain or loss in the sample weight. In some cases, as with Cu-Al-2, the regenerated sample weight is considerably below the base line, but the start of the subsequent sorption is higher. This results from weight gain on exposure to the SO_2-free flue gas prior to sorption.

Weight Gain as an Indication of Sorption

The increasing weight of a sorbent sample was used as a measure of sulfur oxide sorption throughout this study. This method has the advantage of being quick and sensitive, permitting a large number of samples to be evaluated with good reliability. Certain cautions must be exercised, however, to be certain that SO_2 only is contributing to the observed weight gain. For this reason, prior to each sorption run, the sorbent sample was saturated with all the constituents of the flue gas - less SO_2. The actual sorption run corresponded to the time the SO_2 was introduced to the TGA apparatus containing the pretreated sorbent.

As a check, the SO_2 take-up on one sample (Al-12) was compared to actual sulfur analysis. Duplicate sulfur analyses by the Leco method gave results which bracketed the weight gain results and agreed within 15%.

D. Preparation of Sorbents

1. Co-Precipitation

In precipitating the hydroxide or carbonate of a given substance, consideration must be given to the chemistry involved. Some cases are relatively simple, and the combination of any amounts of base and metallic salt will result in precipitation. On the other hand, some substances exhibit amphoteric properties or have soluble complexes, which could interfere with or preclude precipitation. To site a few examples encountered in this study, aluminum hydroxide is amphoteric, copper forms a soluble ammonium complex, and iron hydroxide freshly precipitated with ammonium carbonate is soluble in an excess of the precipitant.

In order to avoid difficulties in co-precipitation which might arise because of these complexes and amphoteric properties, a precipitation titration was made for each metallic ion of interest. To do this, a solution was prepared of the same type and concentration as was to be used in co-precipitation. Using a pH-meter and burette, the pH change with a given quantity of ammonium hydroxide or ammonium carbonate was noted over a wide pH range. At the same time, any changes in appearance, such as precipitate formation, dissolving of the precipitate, or color change, were noted. Having done this, a permissible pH range for the formation of a given precipitate was established. These results are presented in Table VI.

The pH ranges indicated in Table VI are useful guidelines for co-precipitation. To effectively co-precipitate two ionic species, a pH must be selected which is common to the permissible range for each ion. For example, if a co-precipitate of copper and aluminum hydroxides is intended, the range for copper is seen to be 4.6 to 6.8 and that for aluminum 3.9 to 6.4. The overlapping pH range, and the one in which co-precipitation must be made is thus 4.6 to 6.4.

The co-precipitates were separated from the liquid by filtration. The resulting paste-like filter cake was then formed into

Table VI

Precipitation Ranges in NH_4OH and $(NH_4)_2CO_3$

Active Metal Oxides	pH Range	
Metal	NH_4OH	$(NH_4)_2CO_3$
Cu^{II}	4.6 - 6.8	4.6 - 6.0
Zn^{II}	6.6 - 8.0	6.5 - 7.2
Cr^{III}	> 4.6	> 4.2
Mn^{II}	$> \sim 3.0$	> 7.1
Fe^{III}	> 2.6	$\sim 2.5 - \sim 6.6$
Co^{II}	$> \sim 7.5$	7.0 - 7.8
Ni^{II}	7.4 - 8.0	6.6 - 7.8
Supporting Oxides		
Al^{III}	3.9 - 6.4	$4.1 - \sim 7.0+$
Zr^{IV}	2.0 - 4.0	2.0 - 4.0
	Acid titrations (HNO_3)	
Si^{IV}	$< \sim 7.5$	
V^{V}	7.6 - 6.6	

pellets. This pelletizing was done by working the paste into 1/8-inch diameter holes in a 1/8-inch thick aluminum plate. On drying in air at 60°C the pellets shrank and had sufficient strength that they could be removed intact from the holes by gentle rapping of the plates. The pellets were then humidity dried at 90°C dry bulb, 70° wet bulb for 8 hours. This was followed by firing in nitrogen at 650°C for 8 hours.

In this study, the co-precipitated sorbents in the later part of the program, Series III, were prepared under the conditions indicated in Table VI. Some of the earlier co-precipitates in Series I and II were, however, made without the benefit of the guidelines derived from the precipitation titrations discussed above. Series III sorbents may be identified by the sample designation which contains the symbol of the active oxide, the supporting oxide and a sequence number, e.g., Cu-Al-1 for the first series III copper oxide on alumina. Series I sorbents have designations such as Al-8 or Si-12 indicating an alumina support or a silica support. Series II uses similar designations followed by a letter, e.g., Al-8A, Si-12B, etc.

2. Impregnation

Oxides of K, Na, Ni, Zn, Cu, Cr, Mn, and Fe were deposited on a commercial porous carrier, Norton LA-3032 (83% Al_2O_3, 15.3% SiO_2). The support was boiled in solutions of metal nitrate for 8 hours, washed, dried and fired at 650°C to decompose the nitrate. These sorbents were given sample designations I-0 through I-8.

3. Commercially Available Materials

Several commercial materials were tested for SO_2 sorption activity. These were Harshaw Catalyst, 10% CuO in alumina, Florite (Florodin Company) and Linde Mol Sieve 5A.

III. SORBENT STUDIES

1. Copper Oxide-Alumina

a. Thermochemistry

Equilibria for the sorption and regeneration of CuO were computed. Although copper aluminates and silicates are known to exist, no thermodynamic data are available and their influence could not be considered.

The calculated sorption compositions are given in Table VII. The data indicate that at temperatures below 650°C, copper sulfate is formed. The sulfate is $CuO.CuSO_4$. Note that in excess SO_2, the $CuO.CuSO_4$ may further convert to $CuSO_4$. Measured capacities indicate such an event. It is apparent that below about 590°C, dissociation pressure of SO_2 and SO_3 will be less than 0.02% assuming that the sorbent is unsaturated. Thus, at temperatures less than 590°C, removal of SO_2 is 90%. The SO_3 concentration is a maximum of 0.06% at 650°C and declines at higher temperatures.

Table VII

Equilibrium Product Distribution for SO_2 Sorption on Copper Oxide
($0.4\ CuO + 6.0\ H_2O + 14.0\ CO_2 + 0.20\ SO_2 + 3.0\ O_2 + 76.8\ N_2$)

Sorbent	Flue Gas Temperature °C 427	527	627	727	827
A. Mole Fraction in Gas Phase					
CO	0	0	0	0	0
COS	0	0	0	0	0
CO_2	0.1404	0.1404	0.1400	0.1400	0.1400
H_2	0	0	0	0	0
H_2O	0.06020	0.06020	0.06013	0.0600	0.0600
H_2S	0	0	0	0	0
O_2	0.02909	0.02909	0.02923	0.02975	0.02989
SO_2	2.310×10^{-9}	1.909×10^{-6}	3.432×10^{-4}	1.498×10^{-3}	1.785×10^{-3}
SO_3	1.090×10^{-7}	1.124×10^{-5}	4.073×10^{-4}	5.024×10^{-4}	2.150×10^{-4}
S_2	0	0	0	0	0
N_2	0.7703	0.7703	0.7696	0.7682	0.7682
B. Mole Fraction in Condensed Phase					
CuO	2.000×10^{-7}	0.01292	0.5449	1.000	1.000
Cu_2O	0	0	0	0	0
CuS	0	0	0	0	0
$CuSO_4$	0	0	0	0	0
Cu_2SO_5	1.000	0.9871	0.4551	0	0
H_2SO_4	0	0	0	0	0
S	0	0	0	0	0

Regeneration calculations were made by computing the equilibrium products of thermal decomposition of Cu_2SO_5 in air and in nitrogen. The phase Cu_2SO_5 represents the phase formed during equilibrium sorption.

The results of the computations are given in Table VIII. The numbers are meaningful only as long as there is condensed phase Cu_2SO_5 present. Under these conditions the mole fractions of SO_2 and SO_3 in the gas phase are equal to their equilibrium partial pressures over the sulfate.

The partial pressure of SO_2 plus SO_3 is 0.016 atm at 726°C and 0.3 atm at 827°C. Thus, regeneration temperatures of 750°C and higher are indicated if a regenerate gas high in SO_x is desired. The formation of aluminate or silicate might improve the regenerability by stabilizing the oxide form of copper but the absence of thermochemical data leaves this question unanswered.

The thermochemistry of hydrogen reduction of $CuSO_4$ predicts the formation of CuS or Cu_2S. Since it has been demonstrated experimentally (see below) that H_2 regenerated copper-alumina sorbents result in conversion to elemental Cu, it is conjectured that the presence of $CuAl_2O_4$ or $Cu_2Al_2O_4$ stabilizes the oxide. Again, lack of thermochemical data precludes further analysis.

b. Preparation and Evaluation - CuO-Alumina

i. Cu-Al-1

Sorbent Cu-Al-1 was one of the most promising sorbents made in the course of this program. Sorption rate and capacity were found to be completely comparable to alkalized alumina. Loaded sorbent was regenerated both thermally and in hydrogen. The hydrogen regeneration can be made at a much lower temperature than is possible with alkalized alumina, which suggests the possibility of an isothermal sorption regeneration process. As a result of these outstanding features, this sorbent received additional emphasis.

Sorbent Cu-Al-1 was synthesized by vigorously stirring a 1.5 M $(NH_4)2CO_3$ into a mixture of 15% $Cu(NO_3)_2$ and $Al(NO_3)_3$ at room temperature, until pH 5.0 was reached. The blue precipitate indicated that $Cu_3(CO_3)_2(OH)_2$ was the predominant copper compound in the precipitate; however, some green $Cu_2CO_3(OH)_2$ and blue-green $Cu(OH)_2$ may have been present as well. The direction of mixing, $(NH_4)_2CO_3$ into the copper aluminum nitrate solution was chosen in order to avoid the formation of the soluble ammonia complex of copper. This complex would have been formed in the excess of $(NH_4)_2CO_3$, which would have been present until just before reaching the endpoint, had the direction of the mixing been the reverse. The mixture was subsequently "aged" for one hour with frequent stirring. The precipitate was filtered, pelletized, dried and fired as usual.

The resulting dark brown sorbent pellets contained copper, reported as 37.7 wt. % CuO, which would correspond to a potential

Table VIII

Equilibrium Product Distribution for Regeneration of Cu_2SO_5 in Oxygen-Nitrogen Gas
(10 Moles Cu_2SO_5; 0.1 Mole N_2, 0.02 Mole O_2)

	Temperature °C					
	427	527	627	727	827	927
A. Mole Fraction in Gas Phase						
N_2	0.8333	0.8333	0.8332	0.8162	0.4879	6.924×10^{-3}
O_2	0.1667	0.1667	0.1668	0.1677	0.2114	0.2994
SO_2				8.954×10^{-3}	0.2277	0.5961
SO_3				7.128×10^{-3}	0.07290	0.09758
B. Mole Fraction in Solid Phase						
CuO	2.300×10^{-8}	3.460×10^{-7}	1.333×10^{-4}	3.940×10^{-4}	0.01224	1.000
Cu_2O	0	0	0	0	0	0
CuS	0	0	0	0	0	0
$CuSO_4$	0	0	0	0	0	0
Cu_2SO_5	1.000	1.000	0.9999	0.9996	0.9878	0
S	0	0	0	0	0	0
C. Heat of Reaction (kcal/mole Cu_2SO_5)	0	0	0.100	1.400	41.80	69.90
D. Heat of Reaction (Per mole SO_2 + SO_3 regenerated (kcal/atoms)	-	-	150.0	71.00	67.90	69.90

stoichiometric capacity of 30 grams SO_2/100 grams sorbent. The surface area of 242 m^2/gm was also very attractive. The pellets were not particularly strong, however, yielding to modest thumb-nail pressure.

Sorption studies on Cu-Al-1 gave very interesting results. The first basic series of sorptions and regenerations was carried out at 300, 450, and 550°C with regeneration in N_2 at 650°C. Initial rates of greater than 200 hr^{-1} and capacities of 35 gm/100 gm were obtained. The sorption capacity is seen to drop with successive runs, indicating aging. Thermal regeneration rates, however, were higher after the first regeneration, possibly due to the formation of a $CuAl_2O_4$ phase. X-ray analysis indicated only CuO in the fresh sorbent, but the aging effects of 6 cycles resulted in the appearance of $CuAl_2O_4$ and Al_2O_3 phases and slight growth of the CuO grains. A concise record of this basic series of experiments is given in Figure 3.

A porosity analysis was made of fresh Cu-Al-1 by the American Instrument Company using the Aminco 5-7125, 60,000 psi porosimeter. The results showed a total pore volume ($>$ 30 Å) of 0.58 cm^3/gm, a density of 3.92 gm/cm^3 (at 60,000 psi) and a 50% porosity of 0.0076 micron. The distribution of pore sizes is shown in Figure 4. It is interesting to note that about two-thirds of the pore volume is in a sharply defined realm between 30 Å and 90 Å while the other third of the pore volume lies between 0.3 micron and 90 microns. This indicates a possible pore structure in which the net of very fine pores is connected to the outside of the pellet by the larger "feeder" pores. This is generally a very desirable type structure, because of the combination of enhanced pore-diffusion characteristics and accessability of sorption sites.

In an attempt to reduce aging by lowering the regeneration temperature, H_2 regeneration was tried. H_2 regeneration, it was found, reduces the sorbent to Cu. This makes actual regeneration rate measurements based on weight loss difficult to interpret. The half-times, however, are nonetheless significant.

Temperature	Regeneration, Half-Time, min.
300	25
350	9
400	9

The rapid regenerations at 300-350°C suggest the possibility of an isothermal sorption-regeneration cycle where the sorbent is transferred from the flue gas to the regeneration gas with no heating or cooling. This would eliminate heat exchange equipment and heat losses and would result in a much lower regeneration cost than shown in Figure 14 of the phase I final report.[1] This would be especially true at low loadings and the economic optimum loading would be shifted downward.

---

[1] Removal of SO_2 from Flue Gas, Avco Corp., PB 177492, Contract No. PH 86-67-51.

Figure 3

SORPTION/REGENERATION HISTORY OF SORBENT No. Cu-Al-1

Composition 37.7 CuO, 61.38% Al_2O_3

Surface Area, m^2/gm 242

Stoichiometric Capacity, gm SO_2/100 gm sorbent 30

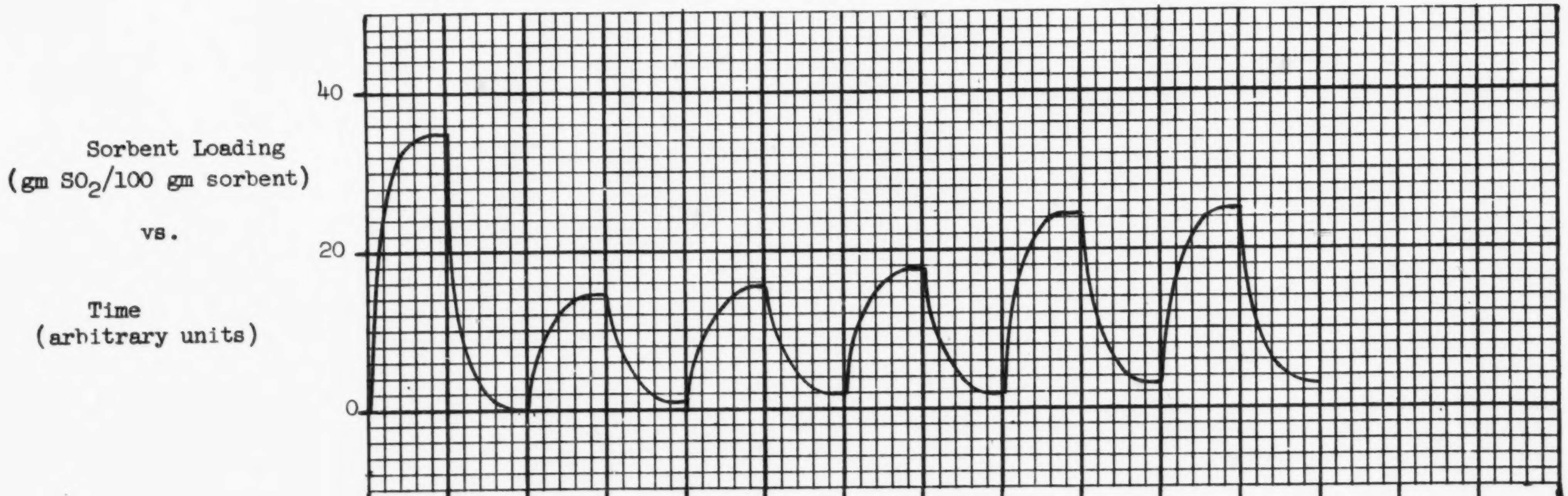

	S1	R1	S2	R2	S3	R3	S4	R4	S5	R5	S6	R6			
Sorption/Regen. Temp., °C	300	650	300	650	450	650	450	650	550	650	550	650			
Initial Normalized Sorption Rate, % loading/% SO_2 hr.	185	-	210	-	260	-	185	-	210	-	185	-			
Ratio Measured/Stoichiom. Cap. %	120	-	49	-	61	-	52	-	76	-	74	-			
Sorption/Regeneration Half-time, min.	40	100	3	7	17	15	12	20	18	25	18	28			

Figure 4

POROSITY DETERMINATION

(By 5-7107 or 5-7108 Aminco—Winslow Porosimeter)

DATE August 6, 1968 Measured Pore Volume: 0.58 cc/g.

SAMPLE Cu-Al-1

WT. OF SAMPLE, G. 0.2194 Measured Density to 60,000 PSI: 3.92 g/cc.

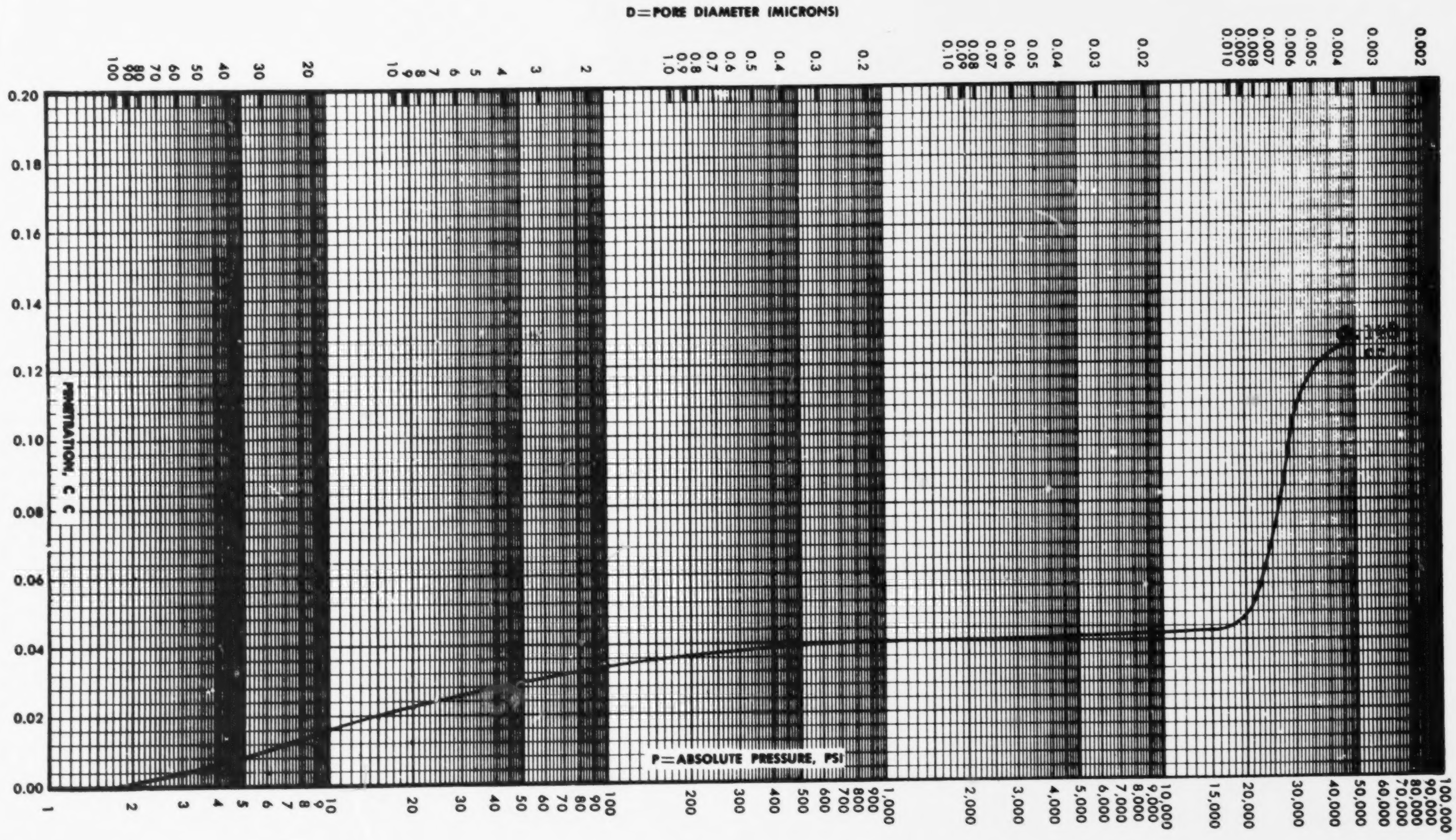

In addition, H_2 regeneration appears to increase sorbent activity, as was demonstrated in the following experiment. A sample was exposed to H_2 for 30 minutes at 300°C, re-oxidizing to reconvert the copper to copper oxide, and then sorbed to saturation in the standard flue gas at 300°C. Subsequent regeneration in H_2 consisted of $2\frac{1}{2}$ hours at 300°C, 3 hours at 325°C and 45 minutes at 350°C. After subsequent re-oxidation, a second sorption at 300°C was made. Again, the sorbent was regenerated in H_2, this time for 50 minutes at 350°C followed by 50 minutes at 375°C. The sample was again reoxidized and a third sorption made at 300°C. The initial rates in these three sorptions increased from about 200 hr^{-1} to 400 hr^{-1}, and finally to over 850 hr^{-1}.

X-ray analysis of the H_2 regenerated material showed no sulfide phases, as would be predicted by thermochemistry, albeit without any knowledge of the influence of the aluminates. There was, however, a strong Cu phase and a weaker phase which might have been $CuAl_2O_4$ or $Cu_2Al_2O_4$. One explanation of this behavior might be the postulated two-step regeneration:

1. $CuO.CuSO_4$, Al_2O_3, and H_2 go to $Cu_2Al_2O_4$, $CuAl_2O_4$, H_2S, and H_2O.
2. $Cu_2Al_2O_4$, $CuAl_2O_4$, and H_2 go to Cu and Al_2O_3.

The second step is presumed to be very much slower than the first and on this basis no Cu will be formed until evolution of H_2S has ceased.

ii. Cu-Al-2

In the preparation of sorbent Cu-Al-2, the intent was to repeat in every detail the preparation of Cu-Al-1. The one exception was that four times as large a quantity of all ingredients was used. Small differences became apparent, however, which deserve some consideration because they are probably significant for all co-precipitations.

Again, 1.5 M $(NH_4)_2CO_3$ was stirred vigorously into a mixture of 15% Cu $(NO_3)_2$ and $Al(NO_3)_3$ at room temperature. Even though the magnetic stirrer and rate of addition were the same, the equivalent amount of carbonate only brought the pH to 4.80 instead of 5.0. Since 4.8 is within the established precipitation range for copper-aluminum, no more carbonate was added. All subsequent treatment was the same as given for Cu-Al-1. The analysis of the finished sorbent Cu-Al-2 showed it contained copper corresponding to 28.9 wt. % CuO and had a surface area of 184 m^2/gm.

Although these differences are not so great that drastically different performance characteristics might be anticipated, they do raise the question of their origin. It is conjectured that the differences stem from subtle differences in the co-precipitation. The mixing characteristics of the 4 times larger volume of liquid resulted in slight differences in the instantaneous pH at the specific point of mixing. This could, for example, have a profound effect on the relative amounts of $Cu_3(CO_3)_2(OH)_2$ and $Cu_2CO_3(OH)_2$ and $Al(OH)_3$ in the co-precipitate. If this hypothesis is true, the significance of this mixing phenomenon for all co-precipitates becomes apparent.

Because of the improved rate and capacity resulting from hydrogen regeneration, it was decided to run the basic sorption series this way for Cu-Al-2. The results of this series are summarized in Figure 5. The unusually high rates, $t_{\frac{1}{2}} = 6.5$ min at 300°C) and saturation loadings (33gm SO_2/100 gm sorbent) make this one of the most promising combinations of this study. As mentioned earlier, it will be noted in Figure 5 that regeneration to constant weight brings the sample weight below the "base line" or original sample weight. This probably is the result of the removal of water and/or other sorbates during regeneration. The start of the subsequent sorption, however, is again above the "base line" since the sorbent is resaturated with SO_2-free flue gas prior to each sorption run.

X-ray diffraction indicated the presence of poorly crystalline $CuAl_2O_4$ and CuO in the unused sorbent.

iii. Al-8A, B, C

These three sorbents, which preceded Cu-Al-2, 2, were co-precipitated under conditions that were similar but not closely controlled. The final copper contents of the sorbents differ markedly from the anticipated, however, again underlining the great importance mixing and localized transitory precipitation conditions. $Cu(NO_3)_3 \cdot 3H_2O$ and $Al(NO_3)_3 \cdot 9H_2O$ were used as starting material for each of these sorbents. The procedure followed for all three sorbents is as follows. The amounts of these substances were computed based on intended levels of copper oxide in the final sorbent. These quantities of starting material, and the actual CuO levels are presented in the following table. (For purposes of comparison, the surface area, which was determined subsequently, is also included in the table.)

Sorbent	Grams of $Cu(NO_3)_2 \cdot 3H_2O$	Grams of $Al(NO_3)_3 \cdot 9H_2O$	wt. % of CuO	Surface Area - m^2/g
Al-8A	7.56	129	11.6	224
Al-8B	22.6	92.3	34.4	74
Al-8C	45.2	37.4	75.3	11

The indicated quantities of copper and aluminum nitrates were dissolved in 200 ml of water at 70°C. Ammonium hydroxide (approximately 0.5 M) was added until the pH reached 6.3; the mixture was allowed to age for two hours at 85°C, and then filtered. The precipitate was washed with distilled water. The paste-like precipitate was then pelletized, dried and fired in the usual manner. The resulting sorbents, Al-8A, B, and C were subjected to the basic sorption series, with a few additional measurements. The results of these tests and the important properties of each sorbent are combined in Figures 6 and 7. The results with Al-8C were sufficiently disappointing that they are not presented here.

Figure 5

SORPTION/REGENERATION HISTORY OF SORBENT No. Cu-Al-2

Composition 28.9% CuO in Al_2O_3

Surface Area, m^2/gm 184

Stoichiometric Capacity, gm SO_2/100 gm sorbent 23.2

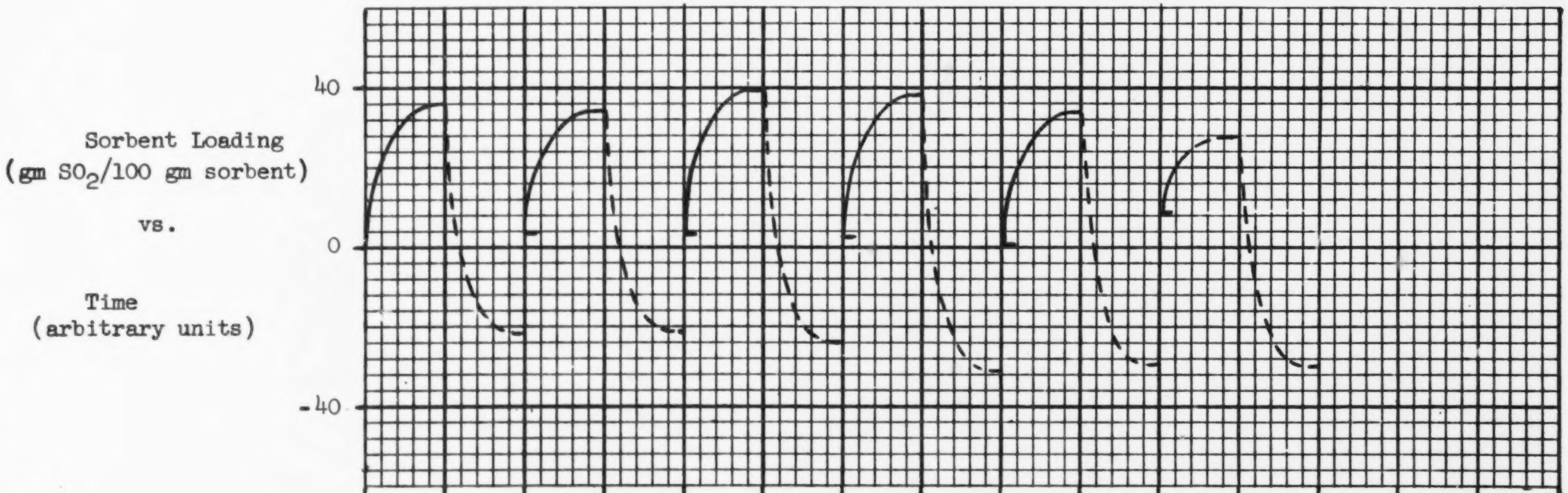

H_2 Regeneration	S1	R1	S2	R2	S3	R3	S4	R4	S5	R5	S6	R6			
Sorption/Regen. Temp., °C	300	400	300	450	450	450	450	450/ 550	550	550	550	550			
Initial Normalized Sorption Rate, % loading/% SO_2 hr.	273	-	317	-	288	-	480	-	859	-	246	-			
Ratio Measured/Stoichiom. Cap. %	154	-	128	-	153	-	151	-	142	-	-	-			
Sorption/Regeneration Half-time, min.	6.7	<5	6.3	<5	5.9	<5	11.5	<5	10.2	<5	-	-			

Figure 6

SORPTION/REGENERATION HISTORY OF SORBENT No. A1-8A

Composition 11.6% CuO in Al_2O_3

Surface Area, m^2/gm 224

Stoichiometric Capacity, gm SO_2/100 gm sorbent 9.03

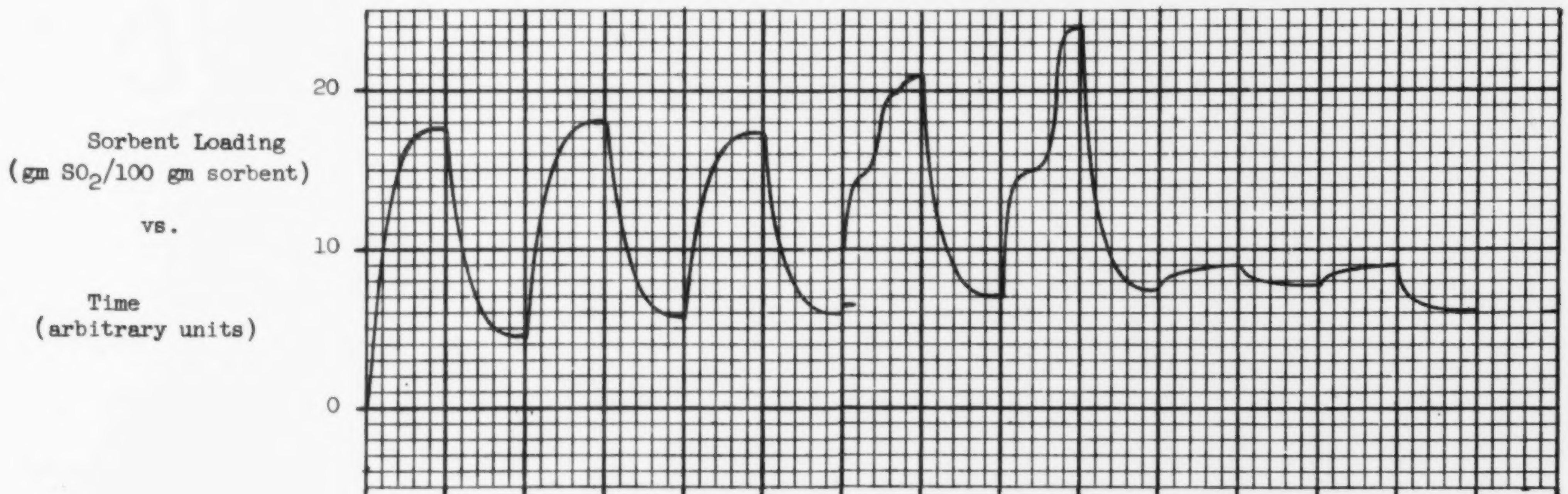

	S1	R1	S2	R2	S3	R3	S4	R4	S5	R5	S6	R6	S7	R7
Sorption/Regen. Temp., °C	300	650	300	650	300	675	450	675	450	675	550	675	550	675
Initial Normalized Sorption Rate, % loading/% SO_2 hr.	197	-	-	-	-	-	171	-	161	-	21	-	35	-
Ratio Measured/Stoichiom. Cap. %	192	-	153	-	127	-	163	-	189	-	24	-	15	-
Sorption/Regeneration Half-time, min.	30	12	37	9	20	8	50	10	65	13	3	7	3	3

Figure 7

SORPTION/REGENERATION HISTORY OF SORBENT No. A1-8B

Composition 34.4% CuO in Al_2O_3

Surface Area, m^2/gm 74

Stoichiometric Capacity, gm SO_2/100 gm sorbent 27.4

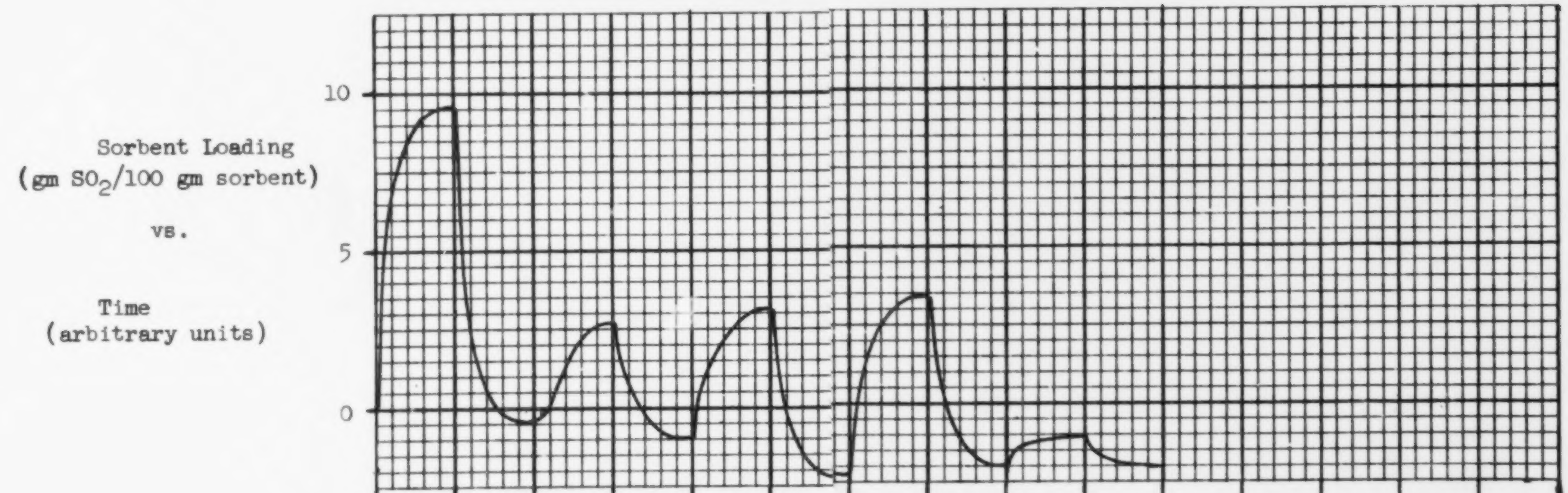

	S1	R1	S2	R2	S3	R3	S4	R4	S5	R5
Sorption/Regen. Temp., °C	300	620	450	600	450	675	450	675	300	675
Initial Normalized Sorption Rate, % loading/% SO_2 hr.	76.6		0		8.2		35.4		12.8	
Ratio Measured/Stoichiom. Cap. %	34		11		10					
Sorption/Regeneration Half-time, min.	25	5	50	50	39	70				

Of the three sorbents, the only one with a high SO_2 capacity was Al-8A, the one lowest in CuO. The first five runs at 300°C and 450°C had an average saturation capacity of about 18 gms SO_2/100 grams sorbent. This is twice the loading that would be expected from the CuO analysis, assuming the sorption proceeds as

$$CuO + SO_2 + \frac{1}{2} O_2 \longrightarrow CuSO_4$$

However, the twice stoichiometric loading might be explained by dithionate formation, but this has not yet been verified. Sorption of moisture and flue gas components other than SO_2 cannot be responsible as these have been measured and are zero at 450°C and less than 4% at 300°C.

Note also that very little capacity was observed at 550°C. This is contrary to the results of the thermochemical calculations which indicate that sorption rather than dissociation should prevail until temperatures of more than 590°C are obtained. However, if sorption does occur by formation of bisulfates or dithionates these calculations no longer apply. No explanation of the "shoulders" in the sorption curves (Fig. 6) for S4 and S5 is apparent.

The ratio of the measured to the stoichiometric capacity [illegible]

at 300°C and 450°C were considered in these averages. It is postulated that this decrease in utilization of potential capacity is a result of the observed decreasing surface area and hence decreasing availability of the CuO.

Attempts to correlate rate data with reaction rate and pore diffusion models were inconclusive. Thus, there is no clear-cut determining process that could be established for sorption on these three sorbents.

iv. Other Copper Oxide Alumina Sorbents

The following sorbents were made and tested, but their performances were not of sufficient significance to merit detailed description: Al-8, I-6, and Harshaw $CuO-Al_2O_3$ catalyst. Available data for these sorbents may be found in Appendix I.

2. Copper Oxide-Silica

a. Thermochemistry

The thermochemistry of this system was considered only in terms of copper, copper oxides, and sulfates. Thus reduced, the thermochemistry becomes the same as has already been discussed for copper oxide-alumina, to which the reader is referred.

b. Preparation and Evaluation - CuO-Silica

Silica supported sorbents can be made by co-precipitation with silica gel, followed by firing. The silica gel, $SiO_2.nH_2O$, is conveniently formed by the reaction

$$Na_2SiO_3 + 2H^+ (n-1)H_2O \longrightarrow SiO_2.nH_2O + 2Na^+$$

The precipitation of the copper constituent is from a solution of a copper salt, such as $CuNO_3$, which is acid because of hydrolysis. This acidity is usually sufficient for the formation of the silica gel. At the same time, Na_2SiO_3 forms a basic solution which causes the precipitation of $Cu(OH)_2$. The overall reaction for these hydrolyses and precipitations is thus:

$$Cu(NO_3)_2 + Na_2SiO_3 + (n + 1)\ H_2O \longrightarrow Cu(OH)_2 + SiO_2.nH_2O + 2NaNO_3$$

Stoichiometric quantities of the reactants yield a sorbent of 57.3 wt. % CuO in SiO_2. Some variation in this ratio can be realized by adjusting the amounts of $Cu(NO_3)_2$ and Ni_2SiO_3. If wider variation of the levels of copper oxide is desired than can be obtained in this fashion, slight pH can be made. Sorbents with low copper content, for example, can be made by adding acid to the copper nitrate solution. If either of these alternatives is to be utilized, however, care must be taken not to exceed the limits of the pH range for co-precipitation, as discussed earlier.

i. Cu-Si-1

This sorbent was prepared by adding 750 ml of 1 M $CuNO_3$ to 630 ml of 1 M Na_2SiO_3 with vigorous stirring at room temperature. The final pH of the mixture was 5.0. After aging, with frequent stirring for 1 hour, the precipitate was separated by filtration. The filter cake was broken up, slurried in 200 ml 0.5 M NH_4NO_3 and re-filtered to remove sodium. After repeating this washing operation three times, the filtrate showed negligible sodium in a flame test. The paste-like precipitate was then pelletized, dried and fired in the usual fashion.

The finished sorbent, Cu-Si-1, was found to have copper corresponding to 59.1% CuO, very close to the 61% predicted from the ratio of reactants in the co-precipitation. The surface area was found to be 97 m^2/gm. This is an attractively high surface area for a sorbent so high in active oxide. As can be seen with other CuO-silica as well as other sorbents, surface area generally drops off with increasing amounts of active oxide.

The sorbent was subjected to the usual basic sorption evaluation series, plus two additional measurements to determine the effect of hydrogen regeneration. This sequence may be seen in Figure 8. The initial sorptions at 300°C showed low loading and slow rate. Subsequent

Figure 8

SORPTION/REGENERATION HISTORY OF SORBENT No. Cu-Si-1

Composition 59.1% CuO in SiO_2

Surface Area, m^2/gm 97

Stoichiometric Capacity, gm SO_2/100 gm sorbent 47.6

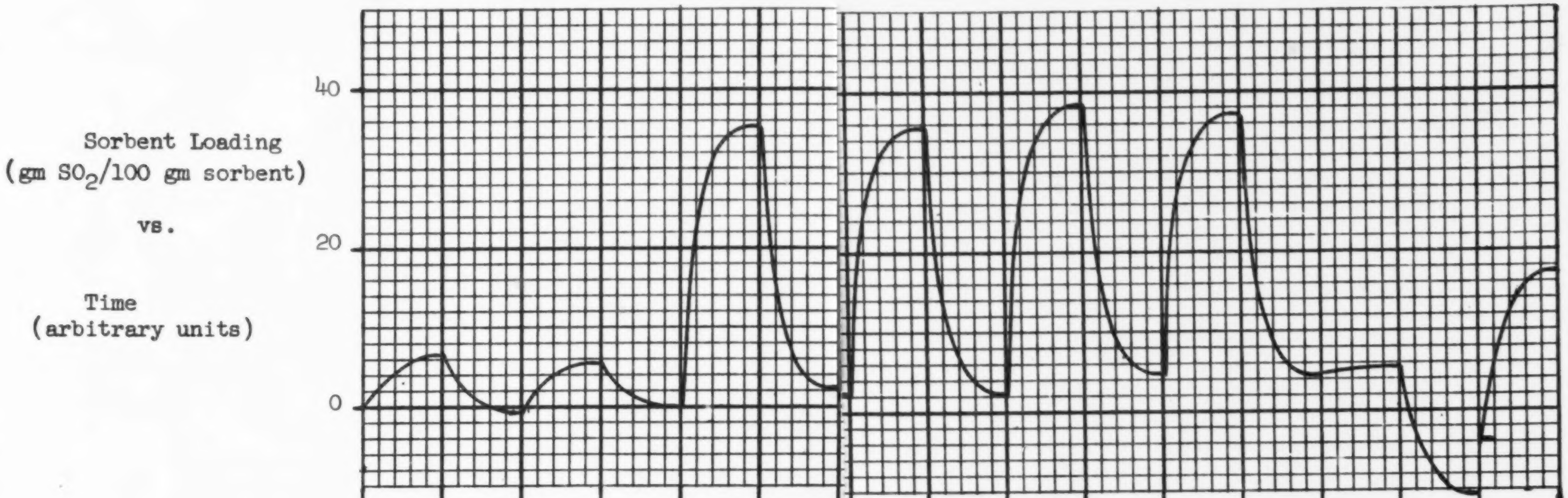

	S1	R1	S2	R2	S3	R3	S4	R4	S5	R5	S6	R6	S7	R7	S8
Sorption/Regen. Temp., °C	300	650	300	650	450	650	450	650	550	650	550	650	300	650/ H_2	30
Initial Normalized Sorption Rate, % loading/% SO_2 hr.	106	-	362	-	894	-	220	-	450	-	350	-	~10	-	~10
Ratio Measured/Stoichiom. Cap. %	13	-	10	-	74	-	69	-	76	-	69	-	3	-	47
Sorption/Regeneration Half-time, min.	77	14	37	14	49	54	32	65	20	100	14	180	23	< 5	190

sorption at 450° and 550°, while much higher in rate and loading, indicate that the sorbent is losing activity with age. To determine the extent of this aging effect, a sorption at 300°C was made subsequent to the basic six. Both rate and loading were found to be much lower than in the first sorptions at 300°, indicating that the sorbent had undergone changes in the first six cycles. After the additional sorption at 300°C, a hydrogen regeneration at 650°C was followed by still another sorption at 300°C. This later sorption showed the same low rate, but the loading was considerably improved. Thus, the beneficial effect of hydrogen regeneration is again demonstrated. Unfortunately, however, little can be deduced from these limited data concerning the cause of these changes in activity.

Attempts to correlate rate data with models for pore diffusion and chemical kinetic were inconclusive for all sorption measurements with this sorbent, due to a high degree of scatter, but the rates and loading were too low to justify an extended treatment of the data.

ii. Si-8A, B, C

These three sorbents were made with three different levels of copper oxide in order to test the effect of this variable. The coprecipitations were made by quickly adding 200 ml of acidified copper nitrate solution to 200 ml of sodium silicate solution at 70°C. The quantities of nitrate, silicate and acid were determined for the desired copper level and a 20 gram yield. After mixing,the pH was adjusted to 5.0 with dilute HNO_3 or NH_4OH and the precipitate "aged" for two hours. Filtering, pelletizing and drying followed the same scheme as outlined in the Introduction. No attempt was made to wash excess sodium from the cake which resulted in 0.7 to 1.5% sodium content in the sorbent.

The amounts of copper nitrate, sodium silicate and concentrated nitric acid used for each sorbent, the CuO level, together with the surface area, are presented for comparison in the following table:

Sorbent	Gram of $Cu(NO_3)_2 \cdot 3H_2O$	Grams of $Na_2SiO_3 \cdot 9H_2O$	cm^2 conc. HNO_3	wt. % CuO	Surface Area, m^2/g
Si-8A	3.03	89.192	38.1	4.75	3.0
Si-8B	9.09	80.5	31.1	14.4	102
Si-8C	27.3	52.1	8.9	43.5	4.5

These sorbents were subjected to the basic sorption series. Si-8A showed essentially zero capacity. The other two sorbents gave good results which are summarized in Figures 9 and 10.

As with alumina based sorbents, the capacities at 300°C and 450°C are good but drop rapidly at 550°C. In contrast with the alumina based sorbents, however, good utilization of the active oxide is obtained at high oxide concentrations, especially at 450°C. Thus, the 45% CuO sorbent

Figure 9

SORPTION/REGENERATION HISTORY OF SORBENT No. Si-8B

Composition 15% CuO in SiO_2

Surface Area, m^2/gm 102

Stoichiometric Capacity, gm SO_2/100 gm sorbent 12

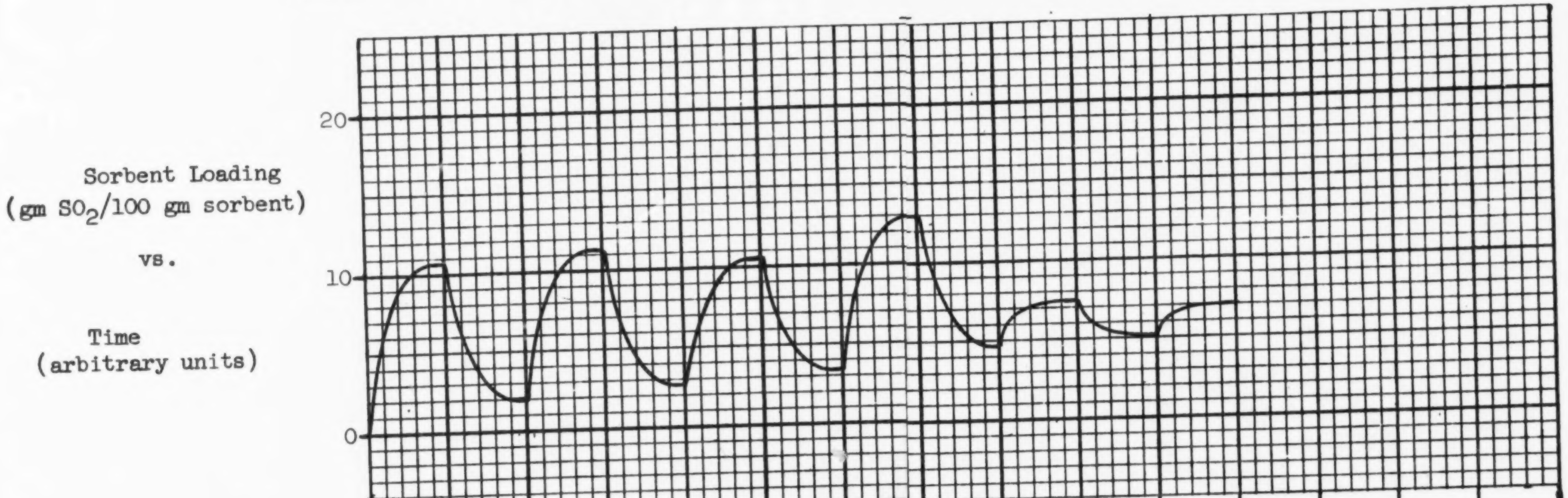

	S1	R1	S2	R2	S3	R3	S4	R4	S5	R5	S6				
Sorption/Regen. Temp., °C	300	650	300	650	450	650	450	650	550	650	550				
Initial Normalized Sorption Rate, % loading/% SO_2 hr.	55	-	51	-	32	-	27	-	230	-	140				
Ratio Measured/Stoichiom. Cap. %	89	-	76	-	63	-	80	-	23	-	23				
Sorption/Regeneration Half-time, min.	24	6	24	12	2.5	-	3.0	10	1.6	-	1.0				

Figure 10

SORPTION/REGENERATION HISTORY OF SORBENT No. Si-8C

Composition 45% CuO in SiO2

Surface Area, m^2/gm 4.5

Stoichiometric Capacity, gm SO_2/100 gm sorbent 36

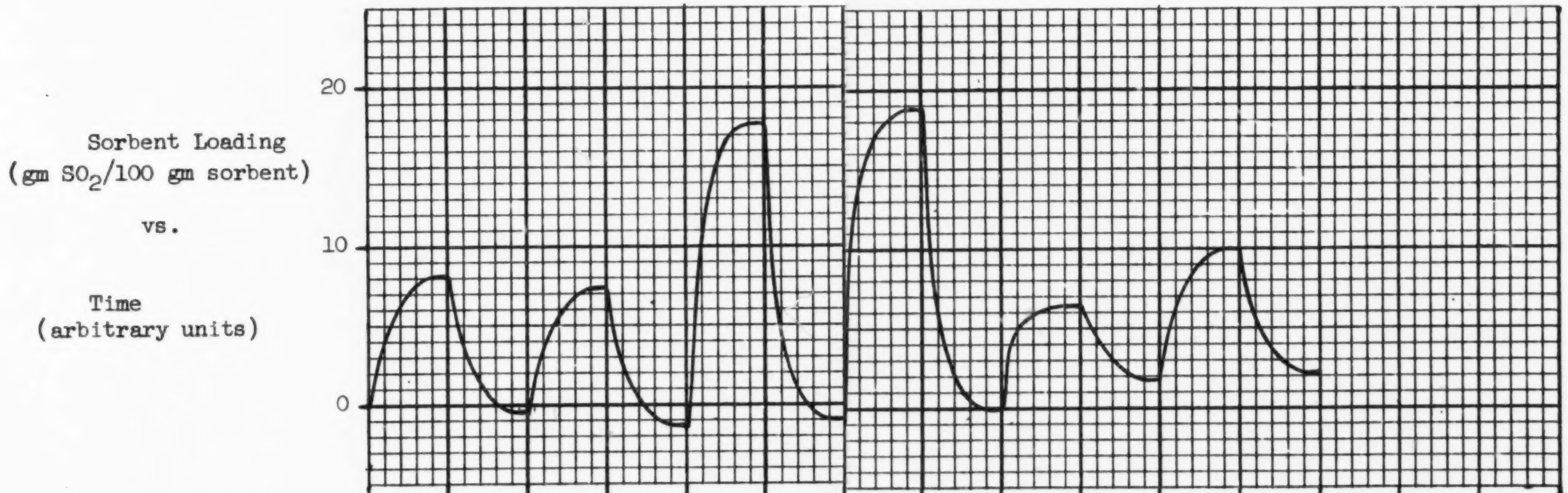

	S1	R1	S2	R2	S3	R3	S4	R4	S5	R5	S6	R6			
Sorption/Regen. Temp., °C	300	650	300	650	450	650	450	650	550	650	550				
Initial Normalized Sorption Rate, % loading/% SO_2 hr.	21	-	10	-	140	-	120	-	210	-	130				
Ratio Measured/Stoichiom. Cap. %	22	-	21	-	48	-	49	-	16	-	20				
Sorption/Regeneration Half-time, min.	51	-	67	18	21	42	20	34	9	27	9	23			

(Si-8C) achieves about half of stoichiometric loading or 18 grams SO_2/100 grams sorbent at 450°C.

Note that the surface area for Si-8B (102 m^2/gms) is higher than for Si-8C and that the ratio of measured to a stoichiometric capacity is also higher, a correlation which has been observed for most of the copper oxide sorbent studies. Thus, as with the copper oxide-alumina sorbents, a higher surface area seems to indicate a higher availability of the active metal oxide.

Increasing sorption temperature from 300° to 450°C increased the rate about tenfold. This is equivalent to an activation energy of about 13 kcal which might correspond to a mixed diffusion-reaction rate controlled sorption or a chemisorption rate controlled sorption.

3. Iron Oxide-Alumina

a. Thermochemistry

Equilibrium computations were made for the sorption (Table IX) and thermal regeneration (Table X) of iron oxide (Fe_2O_3) sorbent. Thermodynamic data for ferrous aluminate were found which permitted its consideration in the computations. The results for the sorption, given in Table IX, show, however, that $FeAl_2O_4$ does not form under the conditions chosen.

The calculations show that the concentration of combined sulfur oxides reaches 0.02% at 475°C. Thus, to achieve 90% removal of sulfur oxides, sorption would have to be carried out at less than this temperature. This constraint is in accordance with the experimental evidence on iron oxide sorbents which indicates a high sorptive capacity at 450°C and almost no capacity at 550°C.

b. Preparation and Evaluation

1. Fe-Al-1

This sorbent was synthesized by co-precipitating with 1.5 M $(NH_4)_2CO_3$ from a solution containing 125 gm $Fe(NO_3)_3 \cdot 9H_2O$ and 184 gm $Al(NO_3)_3 \cdot 9H_2O$ in one liter of water. Because it was determined in the precipitation studies that freshly precipitated $Fe_2O_3 \cdot nH_2O$ is dissolved in excess CO_3, it was necessary to make the co-precipitation by adding the $(NH_4)_2CO_3$ to the mixture of iron and aluminum to a final pH of 6.6, as opposed to adding the iron and aluminum to the carbonate. A large flocculent precipitate was obtained. Before filtering, the precipitate was "aged" for 1 hour, during which period the pH of the mixture drifted to 6.0. This might indicate that more hydroxide was precipitating, or that the initial precipitate was undergoing an exchange reaction from the carbonate to the hydroxide. The material was then filtered, pelletized, dried and fired as usual.

Table IX

Equilibrium Product Distribution for Sorption of SO_2 on Excess Iron Oxide
($0.6667\ Fe_2O_3\ +\ 0.2\ SO_2\ +\ 3.0\ O_2\ +\ 76.8\ N_2\ +\ 14.0\ CO_2\ +\ 6.0\ H_2O$)

	Temperature °C			
	327	427	527	627
A. Mole Fraction in Gas Phase				
CO	0	0	0	0
CO_2	0.1404	0.1404	0.1402	0.1401
H_2	0	0	0	0
H_2O	0.06018	0.06018	0.06009	0.06003
H_2S	0	0	0	0
O_2	0.02909	0.02909	0.02914	0.02914
N_2	0.7703	0.7703	0.7692	0.7684
SO_2	1.103×10^{-10}	4.213×10^{-7}	1.983×10^{-4}	9.145×10^{-4}
SO_3	8.726×10^{-8}	1.986×10^{-5}	1.166×10^{-3}	1.087×10^{-3}
S_2	0	0	0	0
B. Mole Fraction in Solid Phase				
FeO	0	0	0	0
$Fe_{0.94}O$	0	0	0	0
Fe_3O_4	0	0	0	0
Fe_2O_3	0.9000	0.9010	0.9681	1.000
FeS	0	0	0	0
FeS_2	0	0	0	0
$FeSO_4$	0	0	0	0
$Fe_2(SO_4)_3$	0.1000	0.0990	0.03195	0
H_2SO_4	0	0	0	0
S	0	0	0	0

* Both Fe_2SiO_4 and $FeAl_2O_4$ were found not to form.

Table X

Equilibrium Product Distribution for Thermal Regeneration of Ferric Sulfate in Nitrogen
$(1.0\ Fe_2(SO_4)_3\ +\ 1.0\ N_2)$

	Temperature °C				
	427	527	627	727	827
A. Mole Fraction in Gas Phase					
N_2	0.9999	0.9968	0.9246	0.2070	0.1949
O_2	1.094×10^{-5}	6.622×10^{-4}	1.589×10^{-2}	0.1719	0.2203
SO_2	2.200×10^{-5}	1.325×10^{-3}	3.177×10^{-2}	0.[illegible]39	0.4407
SO_3	2.001×10^{-5}	1.171×10^{-3}	2.770×10^{-2}	0.2772	0.1441
S_2	0	0	0		
B. Mole Fraction in Solid Phase					
FeO	0	0	0	0	0
$Fe_{0.94}O$	0	0	0	0	0
Fe_3O_4	0	0	0	0	0
Fe_2O_3	1.399×10^{-5}	8.346×10^{-4}	2.144×10^{-2}	1.000	1.000
FeS	0	0	0	0	0
FeS_2	0	0	0	0	0
$FeSO_4$	0	0	0	0	0
$Fe_2(SO_4)_3$	1.000	0.9992	0.9786	0	0
S	0	0	0		
ΔH_R (kcal/mole $Fe_2(SO_4)_3$)	-0.03	+0.17	+4.00	173.13	185.79

The sorbent was subjected to the first three sorption-regeneration cycles of the "basic sorption series", after which the sequence was interrupted, the sorbent removed, and a fresh sorbent sample (N_2 activated but not previously exposed to flue gas) was introduced to the TGA apparatus. The series was terminated after an additional two cycles. Figure 11 shows this sequence and the results of these measurements. The initial sorption reached a saturation loading of 26.8 grams SO_2/100 grams sorbent which is attractive, but the rate was rather slow - the half-time being about 88 minutes. Subsequent sorption showed a decreasing saturation loading which could be attributed to imperfect regeneration, hydrothermal aging, or the transition to αFe_2O_3. On observing this loss of activity after three cycles, a fresh sample was taken and lower regeneration temperatures, below the αFe_2O_3 transition, were tried. The first sorption with this fresh sorbent (S4) showed a higher rate and saturation loading than had been observed in the third sorption (S3). Subsequent sorption, however, again showed a similar loss of activity, even with the lower regeneration temperature. Thus, this effect cannot be entirely ascribed to the αFe_2O_3 transition.

Analysis of the data of the first sorption (S1) shows that there is a high initial rate, up to the loading of 5 gm/100 gm, followed by a lower rate. The rates at low loading (~5 gm/100) correlate fairly well with the kinetic model suggested in the Phase I, Final Report (ref. 1, pg. 26) for a reaction rate controlling mechanism. For higher loadings the data fit a pore diffusion model. These observations permit two differing explanations. One interpretation is that the pore structure of the sorbent has some large open pores and some very small pores. The larger pores fill quickly and at a rate determined by the chemical reaction; the smaller pores are more slowly filled by a diffusion controlled mechanism. The other interpretation is that if the cause of the loss in activity is related to the structure of the sorbent, some influence might be expected after a few minutes of exposure to flue gas. Further conclusions on this activity decay and possible solutions to the problem would require further experimentation.

ii. Other Iron Oxide Alumina Sorbents

The following sorbents were made and tested but their performances were not of sufficient significance to merit detailed description: Al-12, Al-12A, Al-12B, Al-12C, Al-12D, I-8, and Florite (Floridin Company, Pittsburgh, Pa.).

Additional information may be found in Appendix I.

4. Iron Oxide-Silica

a. Thermochemistry

Equilibrium computations for iron oxide-silica sorbents indicated that no appreciable ferrous silicate formed. The thermochemistry then becomes that of iron oxide-sulfur oxide system. This is treated in the section on iron oxide-alumina sorbents.

Figure 11

SORPTION/REGENERATION HISTORY OF SORBENT No. Fe-Al-1

Composition 45.6% Fe_2O_3 in Al_2O_3

Surface Area, m^2/gm 233

Stoichiometric Capacity, gm SO_2/100 gm sorbent 55

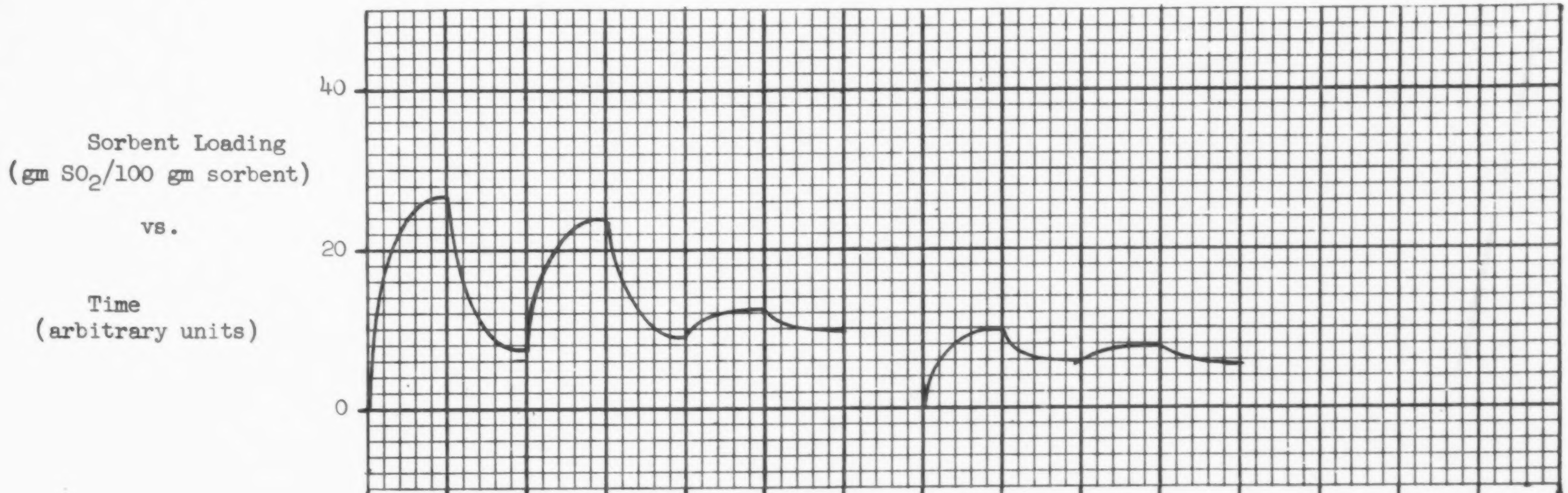

	S1	R1	S2	R2	S3	R3	FRESH SAMPLE	S4	R4	S5	R5				
Sorption/Regen. Temp., °C	300	700	300	700	450	700		450	590	450	590				
Initial Normalized Sorption Rate, % loading/% SO_2 hr.	89	-	80	-	65	-		116	-	38	-				
Ratio Measured/Stoichiom. Cap. %	49	-	30	-	6	-		16	-	2	-				
Sorption/Regeneration Half-time, min.	88	~9	154	~6	8	8		14	12	12	8				

b. Preparation and Evaluation

The precipitation of silica supported sorbents has already been discussed in detail in the section on copper oxide-silica sorbents. For the specific case of iron oxide-silica co-precipitation the overall reaction may be considered to be:

$$2Fe(NO_3)_3 + 3Na_2SiO_3 + (n + m)H_2O \longrightarrow Fe_2O_3.nH_2O + SiO_2.mH_2O + 6NaNO_3$$

As with copper co-precipitates, the proportion of iron in the sorbent may be varied by pH adjustment during precipitation.

i. Fe-Si-1

To one liter of a 0.25 M solution of Na_2SiO_3, increments of a 15 wt. % solution of $FeNO_3$ were added, with vigorous mixing, until the final pH was exactly 7.0. A total of 865 ml of the $Fe(NO_3)_3$ solution was used. The precipitate was then aged for an hour at room temperature, filtered, and washed five times to remove sodium by re-slurrying in 1 M NH_4NO_3 and refiltering. The resulting paste was pelletized, dried, and fired in nitrogen as usual.

The finished sorbent was found to have iron corresponding to 42.5 wt. % Fe_2O_3, which is close to the 47% predicted by the stoichiometry of the chemical equation above. The surface area was quite good, 248 m^2/gram.

The sorbent was subjected to the "basic" sorption series, except that a second sorption at 300°C was omitted since the first one showed no SO_2 sorption. This sequence may be seen in Figure 12. As predicted by the equilibrium computation, SO_2 sorption at 550°C was very low, and at 450°C fairly high, measuring 3 and 22 gram SO_2/100 gram sorbent, respectively. The rates were slow, especially at 450°C where the half-times were about 2 hours. Attempts to correlate the rate data with pore diffusion and reaction models were inconclusive.

ii. Other Iron Oxide Silica Sorbents

The following sorbents were made and tested but their performances were not of sufficient significance to merit detailed discussion: Si-12B, Si-12C, Si-12D.

Available data may be found in Appendix I.

5. Manganese Oxide-Alumina

a. Thermochemistry

The equilibria for sorption and regeneration of manganese oxide sorbents have been computed for a wide variety of conditions and the results compared with available data. The conclusions are as follows:

Figure 12

SORPTION/REGENERATION HISTORY OF SORBENT No. Fe-Si-1

Composition Fe_2O_3 in 57.5% SiO_2

Surface Area, m^2/gm 248

Stoichiometric Capacity, gm SO_2/100 gm sorbent 51

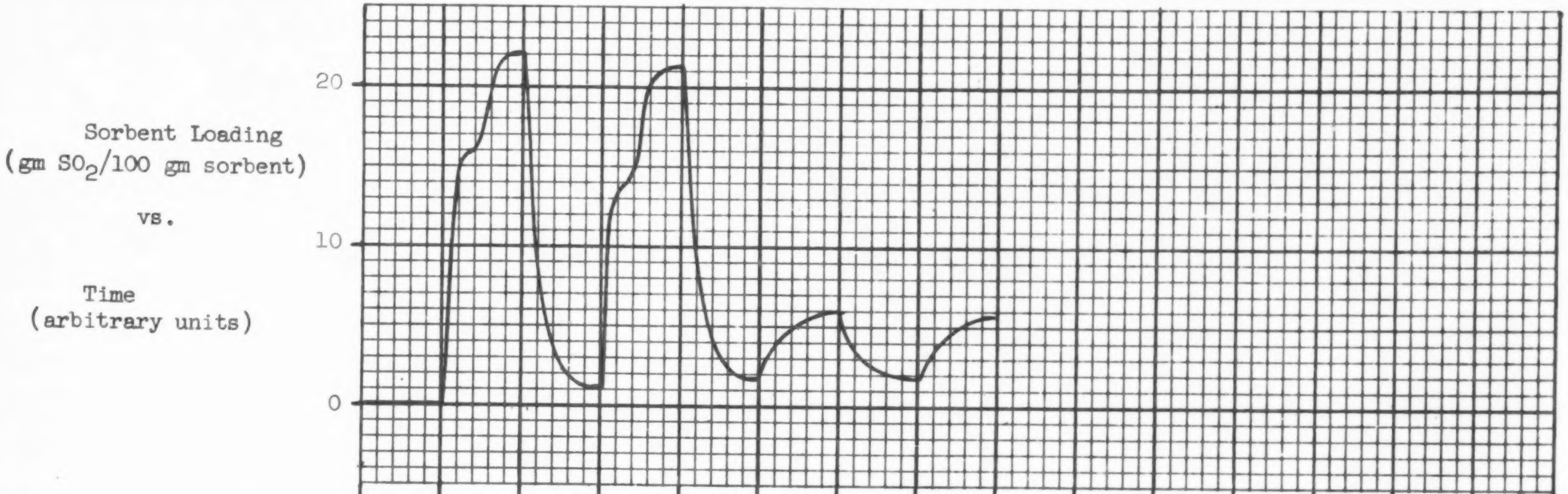

	S1	S2	R2	S3	R3	S4	R4	S5							
Sorption/Regen. Temp., °C	300	450	650	450	650	550	650	550							
Initial Normalized Sorption Rate, % loading/% SO_2 hr.	0	~50	-	~50	-	25	-	23							
Ratio Measured/Stoichiom. Cap. %	0	42	-	39	-	7	-	6							
Sorption/Regeneration Half-time, min.	-	~120	18	120	39	17	11	25							

1. Mn_2O_3 is thermochemically approximately equivalent to Fe_2O_3 and CuO as a sorbent. That is, the partial pressures of SO_2 and SO_3 in a flue gas stream in equilibrium with the sorbents are all similar. The product of sorption is $MnSO_4$.

2. $MnSO_4$ may be thermally regenerated but a temperature on the order of 800°C is required for a partial pressure of SO_2 and SO_3 of 0.1 atm. This is to be compared with 650°C for regeneration of $Fe_2(SO_4)_3$ and 750°C for $CuO.CuSO_4$. Regeneration in steam is essentially equivalent to thermal regeneration.

3. Chemical regeneration of $MnSO_4$ with excess H2, CO $H_2 + H_2O$, and $CO + H_2O$ all yielded a solid with residual MnS as well as MnO or Mn_2O_3 as the regeneration product. Great excesses of $H_2O + H_2$ or $H_2O + CO$ should complete the regeneration, but at the cost of a very dilute off gas.

4. MnO or Mn_2O_3 cannot be stabilized relative to MnS in the presence of a reducing gas by reaction with SiO_2 to form $MnSiO_3$. This results in the formation of MnS during regeneration. Other silicates or zirconates, vanadates, chromates, etc. might stabilize the oxide, but we have been unable to find thermochemical data which would allow checking this point.

5. A two-stage regeneration process was considered in which MnS from H_2 or CO reduction of $MnSO_4$ was exposed to CO_2, H_2O, or $CO_2 + H_2O$. This scheme does not seem practical as large volumes of gas would be required to convert the sulfide to the oxide, resulting in a very low sulfur concentration in the regenerator gas.

Equilibrium computations were made for a sorbent of 0.1 mole Mn_2O_3 in contact with a flue gas consisting of the following components:

CO_2	14.0 mole	O_2	3.0 mole
SO_2	0.2 mole	H_2O	6.0 mole
N_2	76.8 mole		

The distribution of products, computed for the temperature range 327°C to 727°C may be found in Table XI.

It is interesting to note the similarity between these results and those for copper and iron oxide sorbents. For comparison, the temperatures required for 90% removal of the SO_2 initially in the flue gas are 590°C, 590°C, and 475°C for manganese, copper, and iron oxide, respectively.

The possibility of formation of $MnSiO_3$ in a silica-based sorbent was considered, but the formation of this silicate was shown to be thermodynamically unfavorable over the temperature range 327°C to 927°C. This does not rule out the possibility that some other silicate such as Mn_2SiO_5 or $MnSi_2O_5$ might form, but no thermodynamic data could be found for these species. For the same reason, the formation of aluminates, zirconates, or vanadates has not been checked. Both thermal regeneration and regeneration

Table XI

Sorption of Flue Gas on Mn_2O_3
($0.1\ Mn_2O_3 + 6\ H_2O + 14\ CO_2 + 0.2\ SO_2 + 3\ O_2 + 76.8\ N_2$)

	Temperature, °C				
	327	427	527	627	727
A. Mole Fraction in Gas Phase					
N_2	0.7698	0.7698	0.7698	0.7695	0.7682
CO_2	0.1404	0.1404	0.1404	0.1403	0.1400
H_2O	0.06019	0.0619	0.06017	0.06003	0.06001
O_2	0.02961	0.20961	0.02961	0.02962	0.02970
SO_2	$2.813x10^{-12}$	$7.589x10^{-9}$	$2.722x10^{-6}$	$2.536x10^{-4}$	0.001498
SO_3	$2.181x10^{-9}$	$3.590x10^{-7}$	$1.607x10^{-5}$	$3.018x10^{-4}$	0.000502
B. Mole Fraction in Solid Phase					
Mn_2O_3	$5.470x10^{-7}$	$9.139x10^{-5}$	$4.708x10^{-3}$	0.1613	1.0000
Mn_2SO_4	1.000	0.9999	0.9953	0.8387	0.0000

by reducing gas were considered. For regeneration by reducing gas, both one-stage and two-stage procedures were considered.

i. Thermal Regeneration

The equilibrium pressures of SO_2 and SO_3 over $MnSO_4$ were computed for the temperature range of 427°C to 826°C. A mixture of 10 moles $MnSO_4$ and 1 mole of N_2 was considered.

The results of the computations are given in Table XII. The partial pressure of SO_2 plus SO_3 is 0.016 atm at 716°C, 0.1 atm at 800°C, and 0.3 atm at an estimated 860°C. Thus, regeneration temperatures of about 800°C would probably be required to obtain a reasonable regeneration rate. This is higher than the 750°C estimated for thermal regeneration of Cu_2SO_5 and 650°C for $Fe_2(SO_4)_3$.

It was found experimentally that thermal regeneration does not proceed to completion at 600°C. This result is consonant with the computations.

ii. Regeneration with Reducing Gas

Single-stage regeneration with H_2, CO, $H_2 + H_2O$ was considered. In addition, two-stage regeneration in which the $MnSO_4$ was first reduced to MnS and then reacted with H_2O, CO_2 or $H_2O + CO_2$ was considered. Equilibrium computations were made for the temperature range 427°C to 927°C.

One-Stage Regeneration

Regeneration of $MnSO_4$ according to the following reactions was considered.

1. $MnSO_4 + 4H_2 \longrightarrow MnO + 3H_2O + H_2S$
2. $MnSO_4 + 4CO \longrightarrow MnO + 3CO_2 + COS$

Computations were made with 50% excess H_2 and CO and with a 10X excess of H_2. The solid phase was greater than 95 percent MnS at all temperatures when H_2 was the reducing gas and greater than 99 percent when CO was the reducing gas. The remainder of the solid was MnO. There was no difference in the solid composition between a 50-percent excess of H_2 and a 10X excess. Thus, regeneration cannot be effected by great excesses of reducing gas. It appears then that H_2 and CO are unsatisfactory as regenerating gases due to sulfide formation.

The addition of water to the regenerating gas to provide for the conversion of MnS to MnO was also considered. Computations were made for the following cases:

3. $MnSO_4 + 3(H_2 + H_2O)$
4. $MnSO_4 + 9(H_2 + H_2O)$
5. $MnSO_4 + 20(H_2 + H_2O)$
6. $MnSO_4 + 3(CO + H_2O)$
7. $MnSO_4 + 9(CO + H_2O)$
8. $MnSO_4 + 20(CO + H_2O)$

Table XII

$MnSO_4$ Regeneration in Nitrogen
($10\ MnSO_4 + 1.0\ N_2$)

	Temperature, °C				
	427	527	627	727	826
A. Mole Fraction in Gas Phase					
N_2	1.0000	1.0000	0.9988	0.9788	0.7835
O_2	$0.2226x10^{-9}$	$0.5383x10^{-5}$	$0.1999x10^{-3}$	0.00350	0.03487
SO_2	$0.8152x10^{-6}$	$0.2341x10^{-4}$	$0.8864x10^{-3}$	0.01584	0.1605
SO_3	$0.3346x10^{-8}$	$0.1867x10^{-5}$	$0.8669x10^{-4}$	0.001822	0.02107
B. Mole Fraction in Solid Phase					
Mn_2O_3	$4.106x10^{-8}$	$1.269x10^{-6}$	$4.870x10^{-5}$	$9.028x10^{-4}$	$1.173x10^{-2}$
$MnSO_4$	1.000	1.000	1.000	0.9991	0.9883

For case 3, $H_2 + H_2O$, the solid was 54 to 73 mole percent MnS with the remainder being MnO and $MnSO_4$. The presence of $MnSO_4$ was not observed at temperatures equal to or greater than 527°C. For case 6, $CO + H_2O$, the solid phase was 60 to 73 mole percent MnS with the remainder being MnO and $MnSO_4$. The $MnSO_4$ was again a low temperature phase forming between 427°C and 527°C.

For cases 4 and 7, greater excesses of regenerating gas were supplied, and for cases 5 and 8 even more gas was supplied. Case 4 gave a solid phase consisting of 82 mole percent MnS at 927°C increasing to 99 percent at 427°C with the remainder being MnO. No $MnSO_4$ was computed to be formed. The greater excesses of Case 5 gave a solid consisting of 67% MnS at 927°C and 98% at 427°C. Again, the balance of the solid was MnO.

Case 7 gave a solid phase of 90% MnS at 927°C and 99% at 427°C with the remainder as MnO. The greater excess gas in Case 8 gave a solid of 82% MnS at 927°C the balance being MnO. Below 670°C the equilibrium computations indicate the presence of solid carbon.

Thus, increasing the regenerating gas from 6 to 18 moles reduced the conversion to MnO while further increases in the gas to 40 moles effected an increase in MnO. Additional excesses of H_2 or CO plus steam would be expected to completely convert the solid to MnO, at least if the temperature were high enough to prevent $MnSO_4$ or C formation. However, the maximum partial pressure of sulfur compounds for any of the above cases was computed to be less than one mole percent. The regenerate gases would be very dilute in sulfur compounds.

The possibility of regeneration in steam alone was also considered. Computations were made for the following case:

9. $MnSO_4 + 6H_2O$

Above 800°C, the regeneration should proceed well. At 827°C the combined pressure of SO_2 and SO_3 is 0.14 atm. However, at 727°C, the combined pressure is only 0.018 atm. These results differ very little from thermal regeneration in N_2, and the additional hazard of hydrothermal aging would seem to make N_2 regeneration preferable to steam regeneration.

A summary of the results is given in Table XIII. In all cases there is either sulfide formation or, in the case of steam regeneration, no advantage over thermal regeneration. These computational results should be compared with available data and the two reconciled if possible. The experimental work has been largely carried out by the Bureau of Mines at Bruceton.

Bu Mines found that when H_2 or CO was used as the regenerating gas, sulfur removal increased as the temperature was increased from 450°C to 900°C. At 600°C and higher, the solid phases were identified as MnO and MnS. These results are in accord with the equilibrium computations. When regenerating at 450°C, the additional phases $MnSO_4$ and

Table XIII

Summary of Equilibrium Computations for One-Stage Regeneration≠

Case	Results
1. $MnSO_4$ + 6 H_2, 40 H_2	95 mole percent MnS
2. $MnSO_4$ + 6 CO	99 mole percent MnS
3. $MnSO_4$ + 3(H_2 + H_2O)*	54-73% MnS, bal. MnO, $MnSO_4$
4. $MnSO_4$ + 9(H_2 + H_2O)	82-99% MnS, bal. MnO
5. $MnSO_4$ + 20(H_2 + H_2O)	67-98% MnS, bal. MnO
6. $MnSO_4$ + 3(CO + H_2O)*	60-73% MnS, bal. MnO, $MnSO_4$
7. $MnSO_4$ + 9(CO + H_2O)	90-99% MnS, bal. MnO
8. $MnSO_4$ + 20(CO + H_2O)**	82+% MnS, bal. MnO, C
9. $MnSO_4$ + 6H_2O	Mn_2O_3, $MnSO_4$

* $MnSO_4$ present at 427°C calculations but not at 527°C and higher

** C present at 427, 527°C but not at 627°C and above.

≠ When a range of sulfur removal is given the removal increases with temperature

$MnO.Mn_2O_3$ were also formed. The presence of these phases was not predicted by equilibrium and they probably result from kinetic limitations on the reduction of $MnSO_4$ and Mn_2O_3.

When $H_2 + H_2O$ and $CO + H_2O$ were used as regenerating gases, the sulfur removal again increased with temperature. At 600°C and above, the phases MnO and MnS were found. These results are in accord with the equilibrium calculations. At 450°C, the phases $MnSO_4$ and $MnO.Mn_2O_3$ were also identified. The presence of $MnSO_4$ was predicted by the equilibrium calculations, but the Mn_2O_3 is probably present due to the slow rate of reduction at 450°C.

When steam alone was used as the regenerating gas, the sulfur removal again increased with temperature, significant removal occurring at temperatures greater than 750°C as indicated by the equilibrium calculations.

It would appear that the regeneration schemes proposed are all equilibrium limited at reasonable temperatures, either by the formation of MnS or by the low partial pressure of H_2S or COS over the solid. This suggests that it is still important to find a carrier that will react with and stabilize manganese oxide relative to the sulfide, thus allowing the regeneration with H_2, CO, etc. As has been pointed out in previous reports, Al_2O_3 serves this function with an Na_2O sorbent, and in the absence of Al_2O_3, Na_2SO_4 regenerates to Na_2S rather than $NaAlO_2$.

Two-Stage Regeneration with Reducing Gas

All of the one-stage regeneration calculations indicated the presence of residual sulfur as MnS. Thus, it was decided to compute the equilibria for various possible schemes for a second-stage reaction to convert the MnS to MnO or Mn_2O_3. The following second-stage gases were tried: H_2O, CO_2, $H_2O + CO_2$, and air.

Two systems were studied to simulate air regeneration. These were:

10. $MnS + (6\ N_2 + 1.5\ O_2)$
11. $MnS + (12\ N_2 + 3\ O_2)$

For case 10, at temperatures of 527°C and above, the solid phase was entirely MnO and the sulfur was present in the gas entirely as SO_2 at a partial pressure of 0.143 atm. At 427°C, the solid phase has become largely (90 mole percent) MnS and $MnSO_4$ and the partial pressure of SO_2 has dropped to 0.123 atm.

For case 11, in which there is an excess oxygen beyond the requirements for forming SO_3 and Mn_2O_3, the equilibrium is quite different. At temperatures of about 900°C and higher, the solid is entirely Mn_2O_3 and sulfur is present in the gas phase as SO_2 and SO_3 at a combined partial pressure of 0.07 atm. At lower temperatures, the solid becomes largely $MnSO_4$ with decreasing traces of Mn_2O_3. Correspondingly, the partial pressures of SO_2 and SO_3 become very small.

The conclusion to be drawn is that, below 900°C, conversion of MnS to Mn_2O_3 in air will be very slow due to the low equilibrium partial pressures of SO_2 and SO_3. Also, great volumes of air would be required and the sulfur-bearing stream would be as dilute as the flue gas, obviating sulfur recovery. These conclusions are partly confirmed by the BuMines work in which exposure of MnS sorbent to air at 600°C removed only about one-half the sulfur in ten hours.[1]

Mixtures of CO_2 and H_2O have been used to convert alkali sulfides to their oxides. It was felt that this gas mixture should also be considered for conversion of MnS. Equilibria were computed for the following two cases:

12. $MnS + (CO_2 + 2\ H_2O)$

13. $MnS + 3(CO_2 + 2\ H_2O)$

For case 12, the mole fraction of MnO in the solid phase decreased uniformly from 0.026 at 927°C to 0.816×10^{-3} at 427°C. The balance of the solid was MnS. The partial pressure of sulfur bearing gases also decreased from 0.017 atm at 927°C to 0.538×10^{-3} atm at 427°C.

For case 13, the mole fraction of MnO in the solid phase was higher than in case 11 and decreased uniformly from 0.077 at 927°C to 0.0024 at 327°C. The balance was MnS. Again, the pressure of sulfur bearing gases decreased from 0.017 atm to 0.538×10^{-3} atm. Clearly, the use of a sufficient quantity of the H_2O-CO_2 mixture could further convert the MnS to MnO, but, as in the case of air, the sulfur values would be very dilute and non-recoverable.

Finally, computations were made for MnS exposed to pure H_2O and pure CO_2. The following three cases considered for steam regeneration:

14. $MnS + 1.5\ H_2O$

15. $MnS + 4.5\ H_2O$

16. $MnS + 45\ H_2O$

For case 14, the solid phase was 3.1 mole percent MnO at 927°C and 0.12 percent at 427°C. The remainder of the solid was MnS. For case 15, the solid phase was 9.4 percent MnO at 927°C and 0.36 percent at 427°C. For case 16, the solid was 93.6% MnO at 927°C and 3.6% at 427°C. In all cases, the partial pressures of sulfur bearing compounds were 0.0206 atm at 927°C and 0.00081 atm at 427°C. Thus, a sufficient excess of steam should completely remove the sulfur from the solid. This would be done at the cost of a very dilute off gas, however. For the cases at 927°C which gave the highest concentration of sulfur bearing gases, the combined volume percent of H_2S and SO_2 was 2.07. The additional threat of hydrothermal

---

Ref. 1-Bu Mines, Pittsburgh, Quarterly Report to PHS, September 30, 1966.

aging makes steam regeneration appear very unattractive.

Two cases were considered for CO_2 regeneration:

17. $MnS + 1.5\ CO_2$

18. $MnS + 15\ CO_2$

For case 17, the solid was 1.49 mole % MnO at 927°C and 0.0023% at 427°C. For case 18, the solid was 14.9% MnO at 927°C and 0.023% at 427°C. The balance was MnS. For both cases, the partial pressure of sulfur bearing gases was 0.0098 atm at 927°C and 0.000016 atm at 427°C. Thus, the tendency of MnS to convert to MnO in CO_2 as measured by the partial pressure of these gases is less than one tenth that in steam.

In summary, none of the routes examined for the conversion of MnS to MnO_x shows appreciable promise. This result again underlines the importance of discovering a carrier for MnO_x which will stabilize the oxide form relative to the sulfide during regeneration by a reducing gas.

b. Preparation and Evaluation - Manganese Oxide Alumina

i. Mn-Al-1

A solution composed of 150 ml of 15% $Mn(NO_3)_2$ and 275 ml of 15% $Al(NO_3)_3$ was slowly added to 600 ml of 1.5 M $(NH_4)_2CO_3$ at room temperature. The final pH of the mixture was 8.4, somewhat on the high side of the permissible pH range for aluminum precipitation. A substantial precipitate did form, however, which was aged, with frequent stirring, for one hour before filtering. The cake was then pelletized and fired in nitrogen in the usual manner.

The resulting sorbent was extremely weak and tended to powder if handled. For this reason, it was decided to try this synthesis again.

ii. Mn-Al-2

This sorbent was made in exactly the same way as Mn-Al-1 except that the carbonate was added to the mixed nitrates. After mixing in 190 ml of the $(NH_4)_2CO_3$ solution, the pH had reached 5.0 and a very heavy precipitate had formed. Subsequent treatment was the same as with Mn-Al-1.

The resulting sorbent was somewhat stronger than Mn-Al-1, but still showed a tendency to powder. Manganese content corresponded to 37.8% MnO and the surface area was 198 m^2/gram.

The sorbent was subjected to the "basic" sorption series, with the exception that hydrogen was used for regeneration rather than nitrogen. The decision to use hydrogen was based on the results of the thermochemical computation and the poor results with attempts to thermally regenerate previous manganese sorbents.

The sorption-regeneration sequence for Mn-Al-2 may be seen in Figure 13. Good saturation loadings and rates were found at all three temperatures. After the third cycle, however, the slight decline in the initial rates might be an indication of the onset of aging effects. Most of the rate data are sufficiently scattered that no clear-cut interpretation can be made concerning the rate determining mechanism. For both of the sorptions at 550°C, however, a plot of the sorption rate versus sorbent loading is clearly concave downward, indicating that pore diffusion is governing the sorption rate.

iii. Other MnO - Alumina Sorbents

The following sorbents were made and tested but their performances were not sufficiently significant to merit detailed discussion here: Al-9, Al-9A, Al-9B, Al-9C, and I-7.

Additional information may be found in Appendix I.

Figure 13

SORPTION/REGENERATION HISTORY OF SORBENT No. Mn-Al-2

Composition MnO in 62.2% Al_2O_3

Surface Area, m^2/gm 198

Stoichiometric Capacity, gm SO_2/100 gm sorbent 34.0

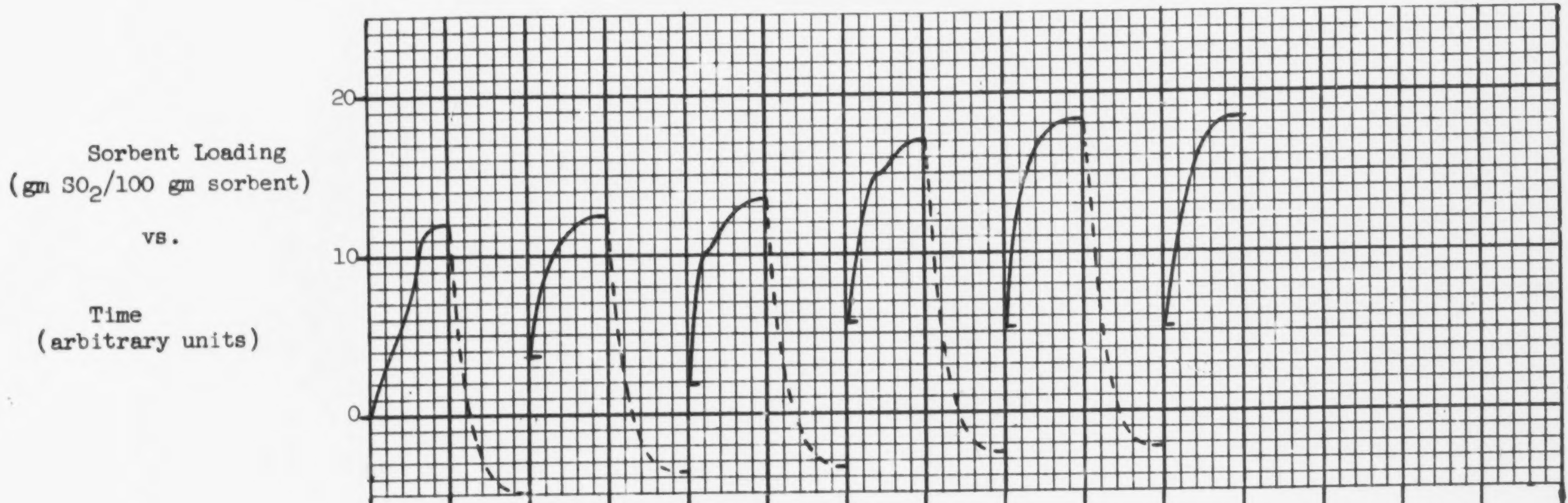

H_2 Regeneration	S1	R1	S2	R2	S3	R3	S4	R4	S5	R5	S6				
Sorption/Regen. Temp., °C	300	650	300	650	450	650	450	650	550	650	550				
Initial Normalized Sorption Rate, % loading/% SO_2 hr.	350	-	445	-	652	-	345	-	286	-	270				
Ratio Measured/Stoichiom. Cap. %	35	-	26	-	34	-	33	-	39	-	39				
Sorption/Regeneration Half-time, min.	12.1	-	13.5	-	10.7	< 5	11.1	< 5	9.4	< 5	9.5				

APPENDIX I

Summary of Sorbents Exhibiting Marginal Performance

For purposes of clarity these sorbents are grouped according to the method of preparation, co-precipitation, impregnation, and those available commercially.

1. Co-Precipitated Sorbents

A large number of sorbents was prepared by this method. These lend themselves to subdivision into three groups, designated Series I, II, III, which correspond to the chronological sequence in which they were made.

a. Series I, Al-1 through Al-14

Oxides of Na, K, Li, Ni, Zn, Cu, Mn, Fe, and Cr were co-precipitated with Al_2O_3. A solution of $Al(NO_3)_3$ and the desired metal nitrate was prepared. This was heated to 70°C and mixed with a solution of $(NH_4)_2\ CO_3$ at the same temperature to cause co-precipitation of the oxides. Great excesses of carbonate ranging from 30 to 150 percent were used. The pH after carbonate addition is estimated to be about 9. The proportions of metal nitrate and $Al(NO_3)_3$ were chosen to match the metal to aluminum ratio desired in the product sorbent. The resulting precipitate was filtered, washed, and the paste spread into a layer on a glass plate, and dried in air for 24 hours at 125°C. The dried material was crushed to approximately the desired 8 mesh size and fired at 650°C in H_2 or N_2.

Note that there was no pH control during precipitation, no uniform mixing procedure, no casting of the precipitate paste before drying to give uniformly shaped pellets, and a rather severe drying schedule.

Chemical analysis, X-ray analysis, and surface area measurements were carried out on sorbents Al-1 through Al-14. The results of these tests are given in Table XIV. In general, the stoichiometric capacities of the sorbents are interestingly high, and with the exception of Al-2, the surface areas are quite high. There is a marked tendency to form aluminates as indicated by the X-ray analysis. Nickel oxide, which showed only a weak aluminate phase as fired (650°C) developed a strong phase where ignited at 1000°C.

The sorbents were tested for SO_2 capacity and regenerability in the TGA apparatus. None was found to have sufficient activity to be of interest.

b. Series II, Al-8A, B, C; Si-8A, B, C; Al-9A, B, C; Al-12B, C, D; Si-12B, C, D

On the basis of the results of Series I sorbents, the more promising oxides of copper, manganese, and iron were chosen for further evaluation.

Table XIV

Properties of Co-Precipitates, Series I

Material	Preparation Conditions Drying Temp. (°C)	Drying Time (hrs)	Firing Temp. (°C)	Firing Time (hrs)	Atm.	Composition (approx. wt. %)	Surface Area (m^2/gm)	Stoichiometric Capacity on Volatile Free Basis (gm SO_2/gm sorb)	X-Ray Diffraction Analysis
Al-1 Li_2O-Al_2O_3 ($LiNO_3$ raw material)	125	24	650	8.8	H_2	14.8% Li_2O	135	0.32	--
Al-2 Li_2O-Al_2O_3 (Li_2SO_4 raw material)			650	5	H_2	13.3% Li_2O 77.0% Al_2O_3	9.6	0.31	$Li_2SO_4 \cdot H_2O$, $LiAl_5O_8$ Al_2O_3
Al-3 K_2O-Al_2O_3	125	24	650	10	H_2	16.7% K_2O 77.1% Al_2O_3 6.2% volatiles	32.3	0.12	--
Al-4 Na_2O-Al_2O_3	125	24	650	10	H_2	8.6% Na_2O 85.5% Al_2O_3 5.9% volatiles	152	0.094	--
Al-5 NiO-Al_2O_3			650	4	N_2	24.7% NiO 65.2% Al_2O_3 9.1% volatiles	275	0.23	NiO Al_2O_3 $NiAl_2O_4$ poorly crystalline
Al-6 Cr_2O_3-Al_2O_3	125	24	650	4.5	N_2	--	131	--	--
Al-7 ZnO-Al_2O_3	125	24	650 650	4 4.8	N_2 H_2	71.6% Al_2O_3 17.0% ZnO 11.5% volatiles	175	.15	$ZnAl_2O_3$ -Al_2O_3 poorly crystalline
Al-8 CuO-Al_2O_3	125	24	650	5	N_2	72.1% Al_2O_3 16.8% CuO 13.5% volatiles	175-220	.15	$CuAl_2O_4$ spinel & -Al_2O_3, CuO(weak) poorly crystalline

Table XIV (Concl'd)

	Preparation Conditions								
	Drying		Firing						
Material	Temp. (°C)	Time (hrs)	Temp. (°C)	Time (hrs)	Atm.	Composition (approx. wt. %)	Surface Area (m^2/gm)	Stoichiometric Capacity on Volatile Free Basis (gm SO_2/gm sorb)	X-Ray Diffraction Analysis
Al-9 $MnO_2-Al_2O_3$	125	24	650	5.5	N_2	98+% Mn_2O_3	--	1.1	--
Al-12 $Fe_2O_3-Al_2O_3$	125	24	650	5	N_2	54.2% Fe_2O_3 34.7% Al_2O_3 11.1% volatiles	146	0.73	Fe_2O_3
Al-14 $Na_2O-MnO_2-Al_2O_3$	125	24	650	8	H_2				
			650	8.5	H_2	--	--	--	--

Each of these active oxides was prepared on an alumina and a silica support. The procedure was as follows:

i. Alumina Based Sorbents

To 200 cc of distilled water were added $Al(NO_3)_3$ and the desired metal nitrate in the proportions desired in the product. Sufficient total salts were dissolved to give 20 grams of product at 100 percent recovery.

The solution was heated to 70°C and NH_4OH solution added to the metal nitrate solution with stirring until the desired pH (as measured with pH paper) was obtained. The precipitate was then aged 2 hours at this pH and 85°C, vacuum filtered, and washed with distilled water. The precipitate, as a thick cake, was pressed into holes of 1/8-inch diameter drilled in an 1/8-inch aluminum plate.

The material was then dried for 1 1/2 hours at 50°C and ambient humidity followed by 2 hours at the controlled humidity of 94°C dry bulb, 74°C wet bulb (in a humidity oven). After this step, the pellets were about 1/16-inch in diameter by 1/16-inch in length. Finally, the pellets were fired in air, heating to 650°C over a period of 2 hours and maintaining at 650°C for 6 hours.

The desired pH to be achieved in the precipitation step was determined ahead of time by separately adding NH_4OH to solutions of $Al(NO_3)_3$ and the other metal nitrate and observing the pH at which precipitation occurred. Short range pH paper was used to determine the pH. The final pH was 6.3 - 6.6 for copper sorbents, 6.0 - 6.4 for manganese, 5.4 - 6.4 for iron.

ii. Silica Based Sorbents

Solutions were prepared of sodium silicate in 200 cc of distilled water and of acidified metal nitrate in 200 cc distilled water. Silicate and metal nitrate were added in the required ratios to give the desired sorbent composition at complete precipitation. Sufficient material was added to produce 20 grams of sorbent at 100 percent yield.

Acidification of the metal nitrate solution was with concentrated HNO_3. Sufficient acid was added so that the two solutions combined would be in stoichiometric balance for the following reactions:

$$M(NO_3)_x + \tfrac{1}{2}x\ Na_2SiO_3 + \tfrac{1}{2}x\ H_2O \longrightarrow M(OH)_x + \tfrac{1}{2}x\ SiO_2 + NaNO_3$$

where M = metal

$$2HNO_3 + Na_2SiO_3 \longrightarrow SiO_2 + H_2O + 2NaNO_3$$

The solutions were warmed to 70°C and the metal nitrate solution added quickly to the silicate. The pH was adjusted to a value of 5 with dilute HNO_3 or NH_4OH and the precipitate digested for 2 hours. Filtering, pelletizing and drying proceeded as with the alumina based materials.

Metal oxide-carrier combinations were prepared and given the following designations:

Metal Oxide	Carrier	
	Al_2O_3	SiO_2
CuO	Al-8A, B, C	Si-8A, B, C
FeO_x	Al-12B, C, D	Si-12B, C, D
MnO_x	Al-9A, B, C	Not Prepared

Chemical analyses and surface areas are given in Table XV.

iii. Sorption-Regeneration Results - Series II

Copper oxide-alumina, Al, 8A, B, C

Copper oxide-silica, Si, 8A, B, C

The results for these sorbents are given in the body of this report (page 37).

Manganese oxide-alumina, Al-9A, B, C

As shown in Table XV, the active oxide content of these sorbents was very low. This accounts for the very low saturation loadings found experimentally.

Iron oxide alumina - Al-12B, C, D

The performances of these sorbents are summarized in Figures 14, 15, and 16. The degrees of utilization demonstrated by these sorbents were low. This is surprising in view of the high surface areas measured (376, 340, 274 cm^2/gm). The highest capacity observed with these sorbents was only about 4 gms SO_2/100 gms sorbent on Al-12-C.

Iron oxide-silica, Si-12B, C, D

Of these sorbents only the data for Si-12B are given (Figure 17) as the saturation capacities for Si-12C and D are less than 5 grams SO_2/100 grams sorbent.

Table XV

Properties of Coprecipitates, Series II

Sorbent	CuO-Alumina			CuO-Silica			Mn_2O_3-Alumina			Fe_2O_3-Alumina			Fe_2O_3-Silica		
Chemical Analysis Wt. %	Al-8A	Al-8B	Al-8C	Si-8A	Si-8B	Si-8C	Al-9A	Al-9B	Al-9C	Al-12B	Al-12C	Al-12D	Si-12B	Si-12C	Si-12D
Active oxide	11.2	34.1	75.3	4.75	14.4	43.5	1.7	2.1	3.2	4.7	13.6	33.4	4.4	10.8	26.8
Al_2O_3 (by dif.)	85.5	65.3	22.7	--	--	--	94.9	76.9	96.0	80.8	77.5	66.4	--	--	--
SiO_2	--	--	--	90.7	83.5	50.6	--	--	--	--	--	--	--	--	--
Na_2O	--	--	--	1.5	0.7	1.2	--	--	--	--	--	--	--	--	--
Volatiles*	3.3 100.0	0.6 100.0	2.0 100.0	0.1 97.1	0.1 98.7	2.0 97.3	3.4 100.0	2.1 100.0	0.8 100.0	14.5 100.0	8.9 100.0	0.2 100.0	0.9	1.5	4.2
Stoichiometric Capacity**															
gm SO_2/100 gm sorbent	9	27	62	3.8	12	45	2.1	3.2	3.9	6.5	18	40	5.2	13	32.2
Surface Area, m^2/gm	224	74	10.5	3.5	102	4.5	304	306	289	376	340	274	163	258	174

* 300°C, 1 hr, He atmosphere

** based on sorbent weight after volatiles removed

Figure 14

SORPTION/REGENERATION HISTORY OF SORBENT No. Al-12B

Composition 4.70% Fe_2O_3 in Al_2O_3

Surface Area, m^2/gm 376

Stoichiometric Capacity, gm SO_2/100 gm sorbent 5.65

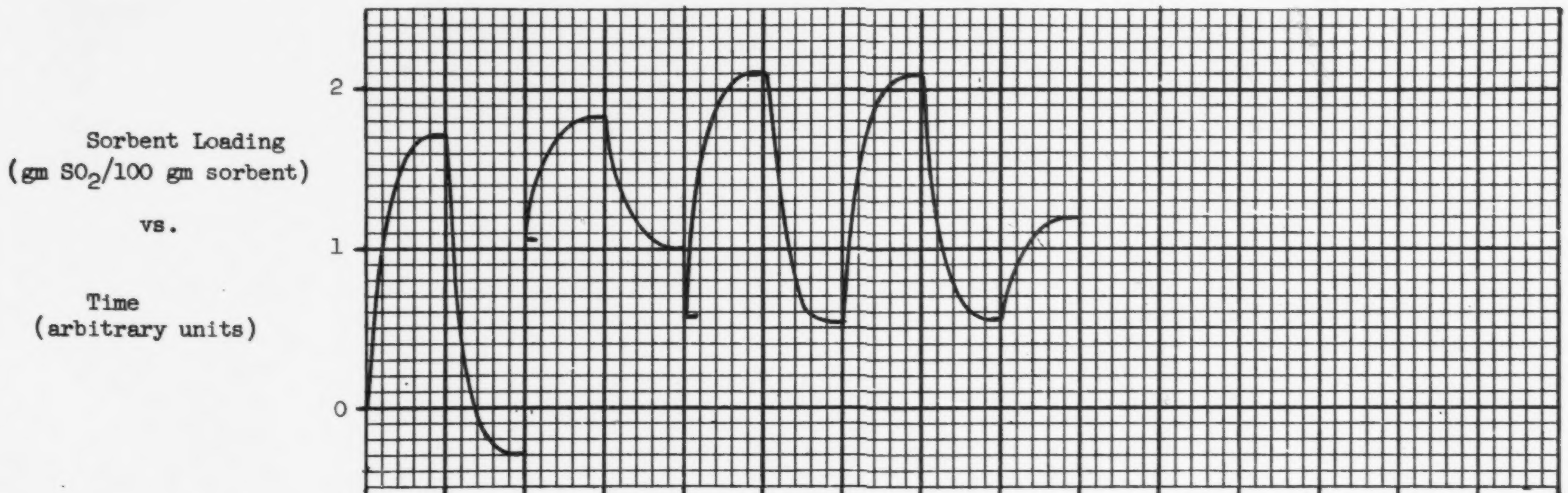

	S1	R1	S2	R2	S3	R3	S4	R4	S5						
Sorption/Regen. Temp., °C	300	750	300	750	450	700	450	750	550						
Initial Normalized Sorption Rate, % loading/% SO_2 hr.	15	-	26	-	43	-	36	-	-						
Ratio Measured/Stoichiom. Cap. %	30	-	13	-	26	-	27	-	11						
Sorption/Regeneration Half-time, min.	10	16	15	-	6	22	6	11	6						

Figure 15

SORPTION/REGENERATION HISTORY OF SORBENT No. Al-12C

Composition 13.6% Fe_2O_3 in Al_2O_3

Surface Area, m^2/gm 340

Stoichiometric Capacity, gm SO_2/100 gm sorbent 16.3

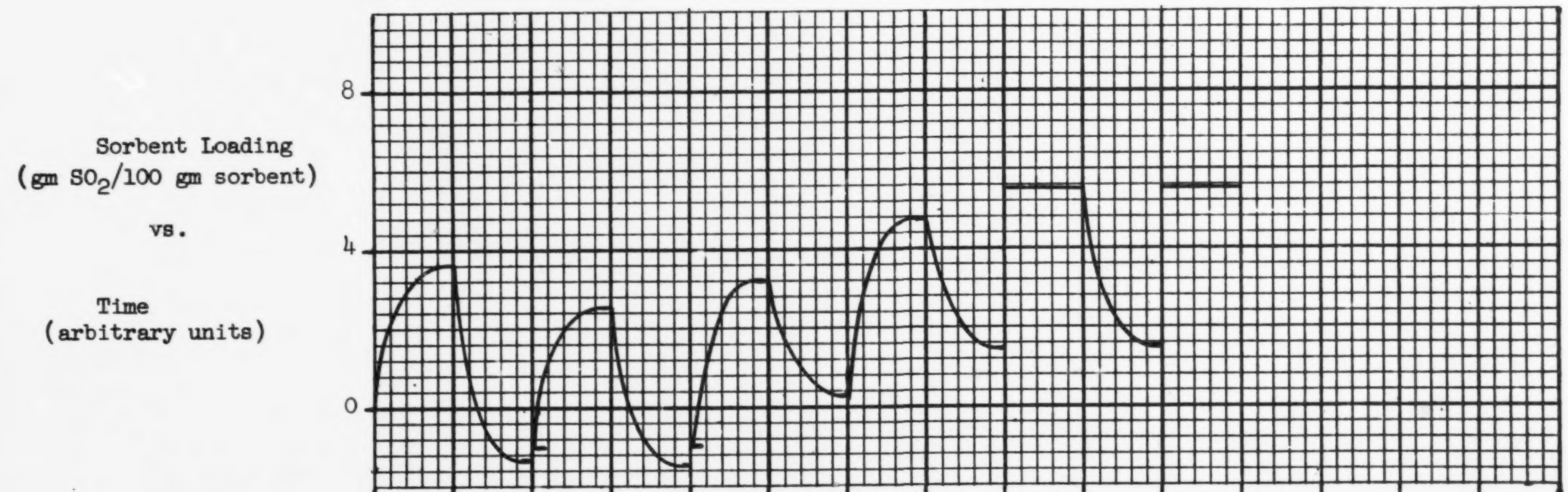

	S1	R1	S2	R2	S3	R3	S4	R4	S5	R5	S6				
Sorption/Regen. Temp., °C	300	650/ 800	300	750	450	750	450	750	500	-	500				
Initial Normalized Sorption Rate, % loading/% SO_2 hr.	55	-	10	-	28	-	23	-	0	-	0				
Ratio Measured/Stoichiom. Cap. %	22	-	21	-	24	-	25	-	0	-	0				
Sorption/Regeneration Half-time, min.	8	-	8	-	17	60	17	70	-	60	-				

Figure 16

SORPTION/REGENERATION HISTORY OF SORBENT No. A1-12D

Composition 33.4% Fe_2O_3 in Al_2O_3

Surface Area, m^2/gm 274

Stoichiometric Capacity, gm SO_2/100 gm sorbent 40.1

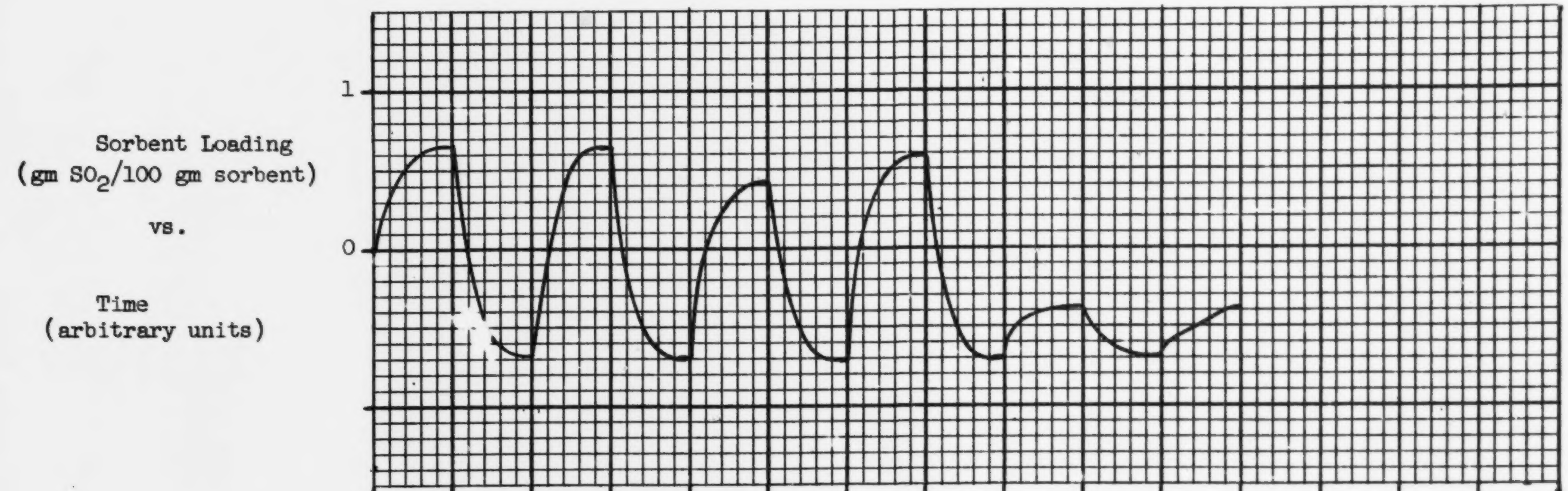

	S1	R1	S2	R2	S3	R3	S4	R4	S5	R5	S6				
Sorption/Regen. Temp., °C	300	700	300	700	450	700	450	700	550	700	550				
Initial Normalized Sorption Rate, % loading/% SO_2 hr.	35	-	17	-	48	-	60	-	20	-	42				
Ratio Measured/Stoichiom. Cap. %	-	-	2	-	3	-	3	-	0.1	-	0.1				
Sorption/Regeneration Half-time, min.	-	-	3	-	5	-	3	-	3	-	2				

Figure 17

SORPTION/REGENERATION HISTORY OF SORBENT No. Si-12B

Composition 4.35% Fe_2O_3 in SiO_2

Surface Area, m^2/gm 163

Stoichiometric Capacity, gm SO_2/100 gm sorbent 5.22

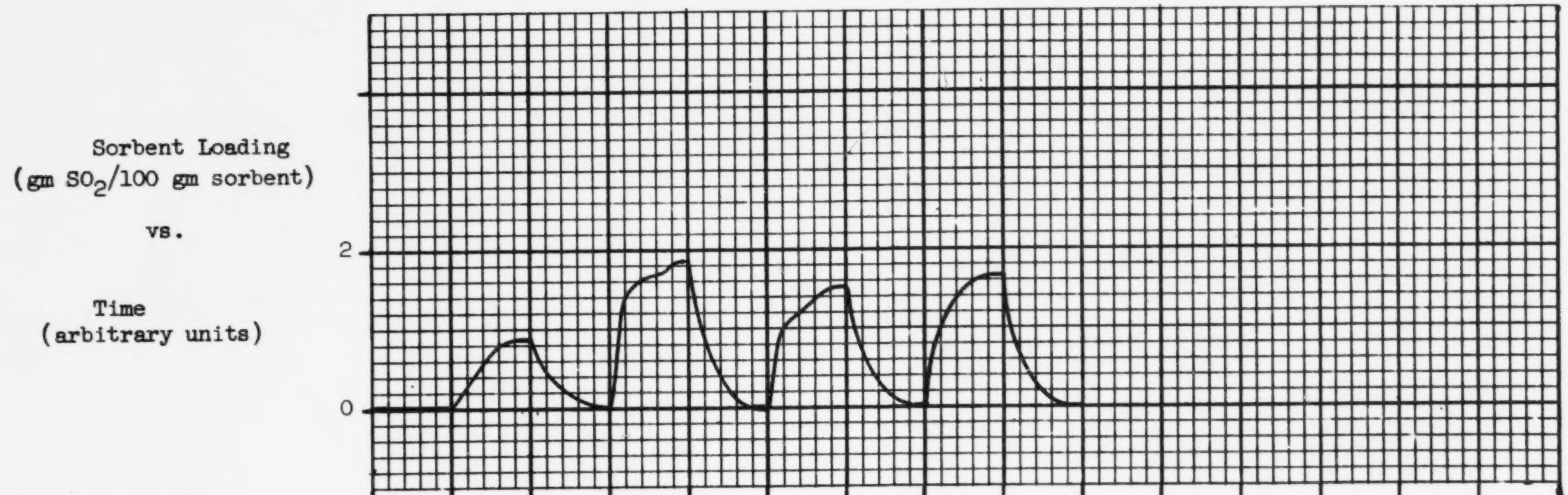

	S1	S2	R2	S3	R3	S4	R4	S5	R5						
Sorption/Regen. Temp., °C	300	450	700	450	700	550	700	550	700						
Initial Normalized Sorption Rate, % loading/% SO_2 hr.	0	5	-	57	-	26	-	37	-						
Ratio Measured/Stoichiom. Cap. %	0	16	-	36	-	29	-	35	-						
Sorption/Regeneration Half-time, min.	-	16	~10	5	~5	6	~3	4	~2						

c. Series III - Cu-V-1, 2; Co-Al-1; Cr-Al-2; Fe-V-1; Fe-Zr-1; Mn-Si-1; Mn-V-1; Ni-Al-1

i. Copper Oxide-Vanadia

The precipitation of $Cu(OH)_2$ and $H_4V_2O_7$ (pyrovanadic acid) from $NaVO_3$ can be represented by the equations:

$$Cu(NO_3)_2 + 2OH^- \longrightarrow Cu(OH)_2 + 2NO_3^-$$

$$2NaVO_3 + 2H^+ + H_2O \longrightarrow H_4V_2O_7 + 2Na^+$$

Since the acid-base requirements of these two reactions are opposite, the co-precipitation of $Cu(OH)_2$ and $H_4V_2O_7$ poses some difficulty. Keeping in mind, however, that because of hydrolysis, $Cu(NO_3)_2$ solution is acidic and $NaVO_3$ solution is basic, the mixing of these two solutions can cause the net reaction:

$$Cu(NO_3)_2 + 2NaVO_3 + 3H_2O \longrightarrow Cu(OH)_2 + H_4V_2O_7 + 2NaNO_3$$

The resultant sorbent, based on this reaction, would have 30.5 wt. % CuO. If sorbents with higher copper content are desired, a larger proportion of $Cu(NO_3)_2$ to $NaVO_3$ must be used, and base or carbonate solutions added to precipitate the additional copper. For lower copper content, additional vanadate and acid must be used.

The first attempt, Cu-V-1, at a sorbent by this scheme was made by slowly adding 15% $Cu(NO_3)_2$ to 1M $NaVO_3$ in the indicated stoichiometric proportions. (1 mole $Ca(NO_3)_2$ to 2 moles $NaVO_3$). The final pH was 4.05 which was more acid than anticipated and it was apparent that precipitation had stopped before half of the copper solution had been added. In hopes of enriching the copper content of the precipitate, 1.5 M $(NH_4)_2CO_3$ was added until pH 5.6 was reached.

This precipitate was stirred for one hour and then filtered. At this point, the precipitate appeared to have a very small particle size and very little was retained in the cake on filtering. The small quantity and chalky appearance led to the decision to try a different approach.

The second attempt, Cu-V-2, utilized the same materials but differed in that the $NaVO_3$ solution was added to the $Cu(NO_3)_2$ solution until a pH of 6.1 was reached. After one hour of stirring, the precipitate was filtered. The quantity and apparent quality of this material was somewhat improved over the previous attempt but it was difficult to filter. This finding, and the modest yield of precipitate led to the decision to forego washing with NH_4 NO_3 solution originally planned to reduce contamination by sodium. Pelletizing and drying were done in the usual manner. On firing in nitrogen at 650°C, the pellets softened and fused together. Possibly it was residual $NaVO_3$ (m.p. 630°C) which melted, or the normal melting point of

V_2O_5 (690°C) may have been lowered somewhat by the presence of sodium or copper salts.

No sorption experiments were attempted with this material.

ii. Cobalt Oxide-Alumina

Only one attempt was made at a sorbent with this combination, which has the designation Co-Al-1. The co-precipitation was made by adding 1.5 M $(NH_4)CO_3$, to a mixture of 15% $Co(NO_3)_2$ plus 15% $Al(NO_3)_3$ to a final pH of 7.3. Here, as with the precipitation of the copper-alumina sorbents, the direction of mixing was chosen in order to reduce possible formation of $Co(NH_3)_6^{++}$. The co-precipitate was, as usual, "aged" for one hour, pelletized, dried and fired in the usual manner.

The finished sorbent was subjected to part of the basic sorption series; the sorptions at 550°C being omitted because of the less than encouraging results at the two lower temperatures. Saturation loading varied between 3.5 and 5.4 gram SO_2/100 grams sorbent which is somewhat surprising in light of the high surface area (171 m^2/gm) and cobalt content corresponding to 49% CoO.

Figure 18 shows the history of the sorption-regeneration sequence. The increasing regenerated sample weight, or shifting base line is quite apparent, and accounts for an increase of over 9% in the four cycles. The oxidation of CoO to Co_2O_3 could at most account for 5.2%. Another possibility could be the formation of $Co_2(SO_4)_3$ which is probably less readily regenerated thermally. Unfortunately, there is insufficient information to support this conjecture.

iii. Chromium Oxide-Alumina

Sorbent Cr-Al-1 was made by adding a solution containing approximately 15% $Cr(NO_3)_2$ and $Al(NO_3)_3$, in a proportion calculated to yield 50 wt. % Cr_2O_3 in the sorbent, to a 1.5 M solution of $(NH_4)_2CO_3$. The final pH was 8.2. The addition of the mixed metallic nitrate solution to the carbonate was considered advantageous because it provided for an excess of carbonate throughout the precipitation. The blue-gray precipitate was aged for one hour before filtering and pelletizing. After air drying at 60°C, humidity drying at 90°C/70°C - dry bulb/wet bulb (in a humidity oven), the pellets were dried in N_2 at 650°C. The resulting sorbent was extremely weak and the pellets crushed to a powder under the lightest touch. The color, a mixture of dark green and black, indicates that the chromia content might be quite high.

Because of these poor structural properties, a second attempt was made using half the amount of $Cr(NO_3)_3$. In precipitating Cr-Al-2, a 1.5 M $(NH_4)_2CO_3$ was added with vigorous stirring to mixed chromium and aluminum nitrates until a pH of 7.2 was reached. After the same filtering,

Figure 18

SORPTION/REGENERATION HISTORY OF SORBENT No. Co-Al-1

Composition 49% CoO in Al_2O_3

Surface Area, m^2/gm 171

Stoichiometric Capacity, gm SO_2/100 gm sorbent 84

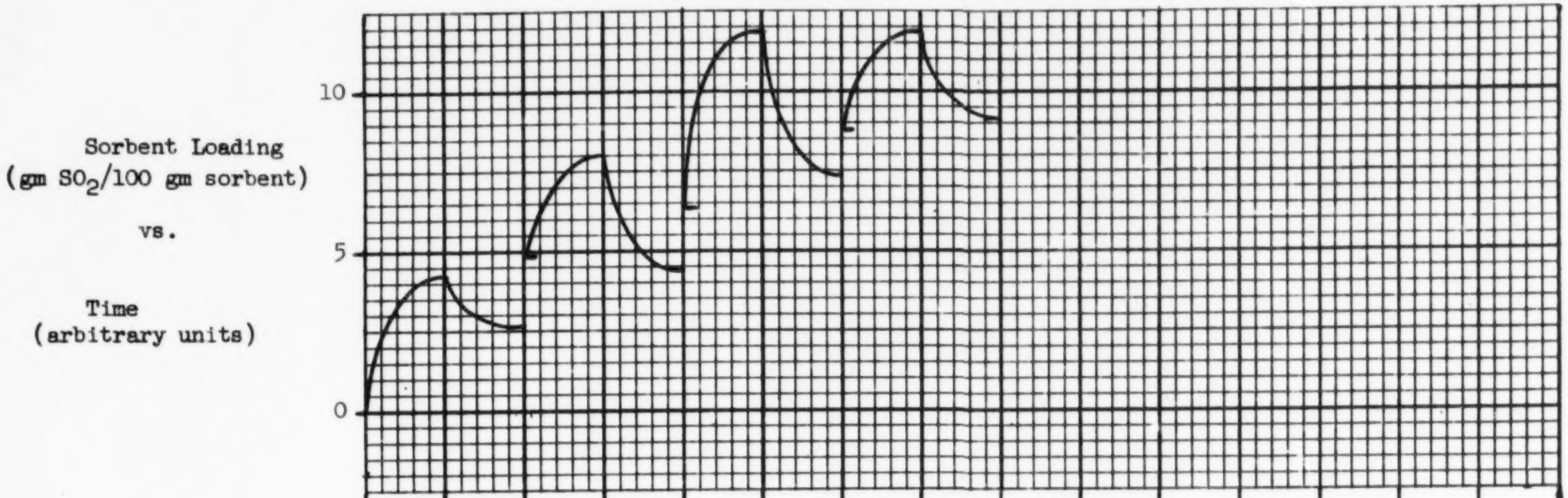

	S1	R1	S2	R2	S3	R3	S4	R4							
Sorption/Regen. Temp., °C	300	650	300	650	450	650	450	650							
Initial Normalized Sorption Rate, % loading/% SO_2 hr.	104	-	74	-	150	-	100	-							
Ratio Measured/Stoichiom. Cap. %	5	-	4	-	6	-	4	-							
Sorption/Regeneration Half-time, min.	12	16	14	21	6	7	4	9							

pelletizing, drying, and firing sequence as with Cr-Al-1, the physical properties of the pellets were not markedly improved. No sorption experiments were attempted with either Cr-Al-1 or Cr-Al-2.

iv. Iron Oxide-Vanadia

The source of vanadia in this combination makes use of the reaction

$$2NaVO_3 + 2H_2O + 2H^+ \longrightarrow H_4V_2O_7 + 2Na^+$$

which yields a gel-like precipitate. Since a solution of $Fe(NO_3)_3$ is quite acid because of hydrolysis, it can effect the above reaction. At the same time, $NaVO_3$ yields a basic solution and hence can precipitate "iron hydroxide", $Fe_2O_3 \cdot H_2O$. The overall reaction for these hydrolyses and precipitations may be written

$$2Fe(NO_3)_3 + 6NaVO_3 + (6 + n)H_2O \longrightarrow Fe_2O_3 \cdot nH_2O + 3H_4V_2O_7 + 6NaVO_3$$

Based on this stoichiometry, the final sorbent should have 22.7% Fe_2O_3 by weight. If other levels of iron are desired, addition of acid to the iron solution (to yield lower Fe_2O_3) or base to the vanadate (to yield higher Fe_2O_3) before mixing would be possible. The iron oxide-vanadia sorbent, Fe-V-1 was made by adding a 1.0 M solution of $NaVO_3$ to a 15% solution of $Fe(NO_3)_3$ until a pH of 5.65 was reached. The precipitate was aged for one hour, then filtered and the cake washed by slurrying in 200 ml of 0.5 M NH_4NO_3 and refiltered. This washing operation was repeated 5 times even though the filtrate from the third washing showed only very weak flame tested for sodium.

The washed precipitate was pelletized, dried and fired in the usual way.

The resultant sorbent showed an iron content on analysis corresponding to 52.7 wt. % Fe_2O_3. The pellets were extremely strong and would appear to be highly attrition resistant. Unfortunately, however, the surface area was found to be only 1.1 m^2/gm. On exposure to a simulated flue gas, no weight gain was observed at 300, 450, or 550°C. In the hope that hydrogen might activate the sorbent, the sorbent was exposed to hydrogen at 550°C for one hour. Subsequent exposure to flue gas resulted in a weight gain corresponding to a low 0.4 gm SO_2/100 gram sorbent.

v. Iron Oxide-Zirconia

Hydrated zirconium oxide is precipitated from alkaline solution as a hydrogel by the reaction

$$ZrOCl_2 + 3H_2O \xrightarrow{OH^-} ZrO_2 \cdot 2H_2O + 2HCl$$

This reaction lends itself to the formation of zirconia based sorbents.

The iron oxide-zirconia sorbent, Fe-Zr-1, was made by slowly adding 1.5 M $(NH_4)_2CO_3$ to a mixture of 0.3 M $Fe(NO_3)_3$ and 0.25 M $ZrOCl_2$, at room temperature until the pH reached 6.0. The voluminous, heavy precipitate was "aged" with frequent stirring, for one hour before filtering. The cake was pelletized, dried and fired in nitrogen as usual.

The resulting sorbent was found to have iron corresponding to 33.6% Fe_2O_3 and a surface area of 272 m^2/gm. Porosity determination, by mercury intrusion, showed the sorbent to have an appreciable pore volume, 0.73 cm^3/gram, between 0.003 and 0.04 microns. Additional pores, smaller than 0.003 micron (30 Å) were also present but could not be measured in the test equipment used. The pore size distribution curve may be seen in Figure 19.

The sorbent was subjected to simulated flue gas at 300°C, 450°C, and 550°C. The saturation loading at 300°C was not especially good and declined at the higher temperatures. As seen in Figure 20, the sorbent also became increasingly difficult to regenerate, and after three cycles its activity was reduced to nearly zero. No further experiments were undertaken.

vi. Manganese Oxide-Silica

The co-precipitation of this combination poses problems similar to those discussed for $CuO-V_2O_5$. By analogy, the net reaction,

$$Mn(NO_3)_2 + Na_2SiO_3 + (n + 1)H_2O \longrightarrow Mn(OH)_2 + SiO_2 \cdot nH_2O + 2NaNO_3$$

might be useful in making this sorbent. Following this approach, a 15% solution of $Mn(NO_3)_2$ was added to a 0.25 M solution of Na_2SiO_3 in a proportion calculated to ultimately yield a sorbent of 50 wt. % MnO in SiO_2. The pH of the resulting mixture was 8.9 which is much too alkaline to precipitate the silica. The pH was, therefore, adjusted to 6.9 with 3 M HNO_3. This precipitate was then filtered and washed five times in 0.5 M NH_4NO_3 to remove traces of sodium. The filter cake was then pelletized, dried and fired in the usual fashion.

The resultant sorbent, Mn-Si-1, was found to contain manganese corresponding to 39 wt. % MnO and a surface area of 36 m^2/gm. In the standardized sorption experiments, the resulting sorbent showed zero capacity for SO_2 at 300°C and 450°C. A slight weight gain in a sorption at 550°C could not be removed by regeneration at 650°C.

vii. Manganese Oxide-Vanadia

The vanadia support for this sorbent was realized by the precipitation of vanadic acid ($H_4V_2O_7$), as was described for the iron oxide vanadia sorbent Fe-V-1.

Sorbent Mn-V-1 was co-precipitated by vigorously mixing 700 ml of solution containing 252 grams of $Mn(NO_3)_2$ into 1.4 liters containing 172 grams of $NaVO_3$. The heavy gelatenous precipitate was aged with frequent stirring for one hour and then filtered. To remove sodium, the filter cake

Figure 19

POROSITY DETERMINATION

(By 5-7107 or 5-7108 Aminco—Winslow Porosimeter)

DATE August 6, 1968 Measured Pore Volume: 0.73 cc/g.

SAMPLE Fe-Zr-1

WT. OF SAMPLE, G. 0.3020 Measured Density to 60,000 PSI: 2.79 g/c

0.219 cc

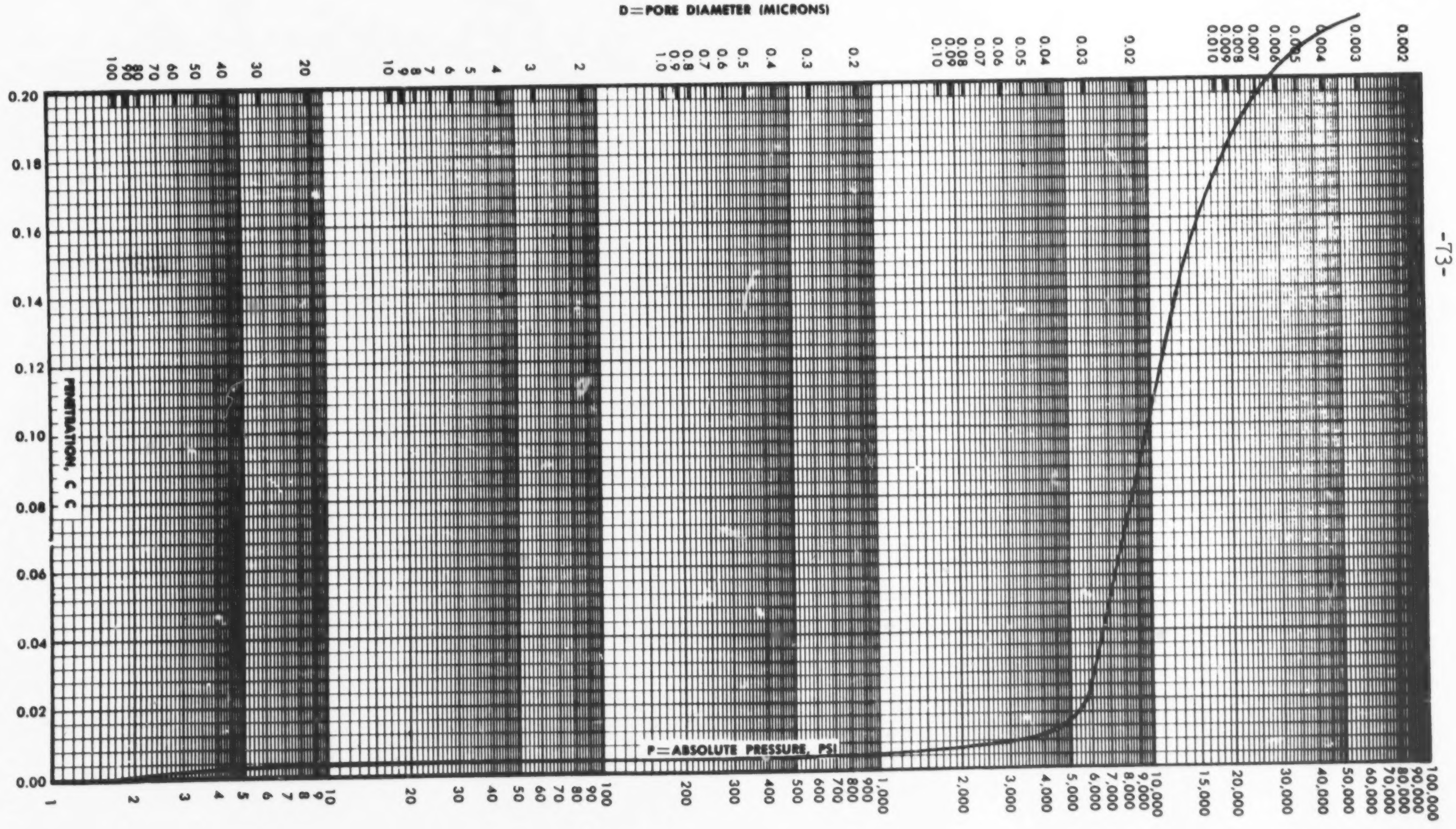

Figure 20

SORPTION/REGENERATION HISTORY OF SORBENT No. Fe-Zr-1

Composition 33.6% Fe_2O_3 in ZrO_2

Surface Area, m^2/gm 272

Stoichiometric Capacity, gm SO_2/100 gm sorbent 40.4

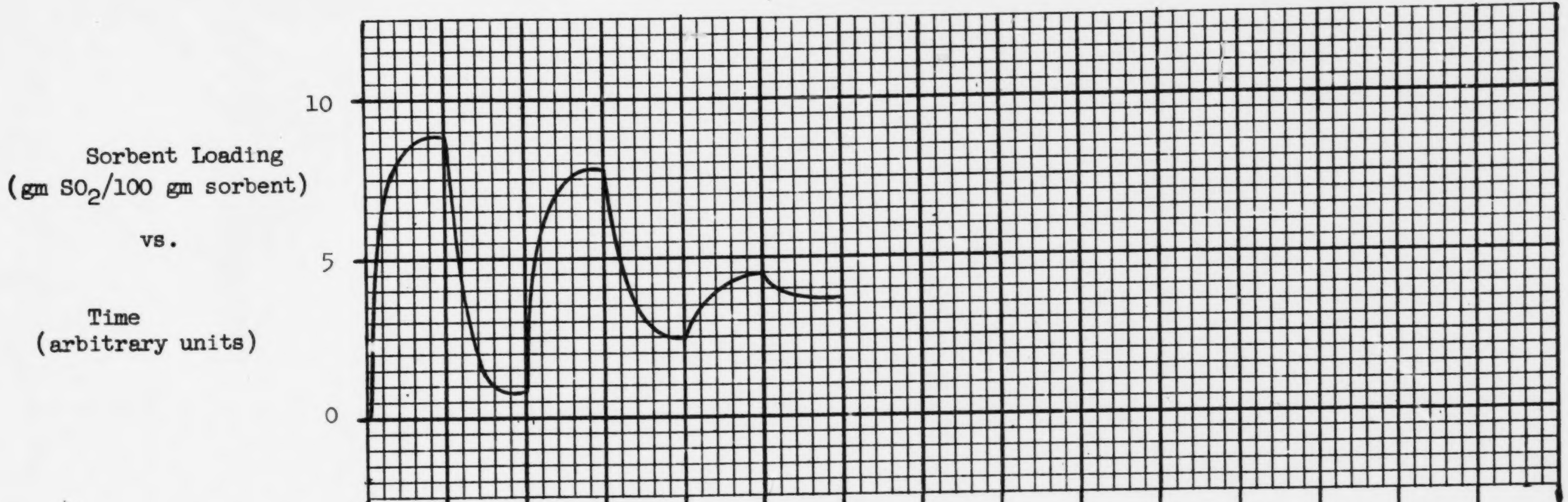

	S1	R1	S2	R2	S3	R3
Sorption/Regen. Temp., °C	300	600	450	600	550	600
Initial Normalized Sorption Rate, % loading/% SO_2 hr.	10	-	129	-	61	-
Ratio Measured/Stoichiom. Cap. %	22	-	16	-	6	-
Sorption/Regeneration Half-time, min.	105	8	14	3	4	8

was washed five times by reslurrying in 0.5 M NH_4NO_3 and refiltering. The washed co-precipitate was pelletized, dried and fired as usual.

The resultant sorbent was found to have manganese content corresponding to 62.1% MnO and surface area of 1.1 m^2/g.

On exposure to simulated flue gas, the saturation loadings of 0.83 at 300°C, 10.2 and 4.2 at 450°C and 3.4 grams SO_2/100 grams sorbent at 450°C were measured.

viii. Nickel Oxide-Alumina

Co-precipitation was made by adding a total of 2000 ml of 1.5 M $(NH_4)_2CO_3$ to a solution containing 195 grams $Ni(NO_3)_2 \cdot 6H_2O$ and 371 grams $Al(NO_3)_3 \cdot 9H_2O$ in 1500 ml water. The final pH of the mixture was 6.3. After aging for one hour, the precipitate was filtered and the cake pelletized. The pellets were then air dried at 60°C and humidity dried at 90°C dry bulb, 70°C wet bulb temperature, before firing for eight hours in nitrogen at 650°C.

The resultant sorbent, Ni-Al-1, was analyzed and found to contain nickel corresponding to 26.4 wt. % NiO and surface area of 306 m^2/gm.

On exposure to simulated flue gas, saturation loadings of 4.3, 2.6 and 2.7 gram SO_2/100 gram sorbent at 330°C, 450°C, and 550°C were observed. This sequence of sorptions and regenerations may be seen in Figure 21.

2. Sorbents Made by Impregnation

Oxides of K, Na, Ni, Zn, Cu, Cr, Mn, and Fe were deposited on a commercial porous carrier, Norton 3032, 83% Al_2O_3, 15.3% SiO_2. The support was boiled in solutions of metal nitrate for 8 hours, washed, dried and fired at 650°C to decompose the nitrate. Nine sorbents were so prepared. They are designated I-0 through I-8.

Chemical, X-ray and surface area analyses were carried out on these samples. The results of these tests are given in Table XVI. Generally the surface area of the impregnated sorbent was slightly less than that of the carrier, but still high. X-ray analysis showed only weak lines at best for the added metal oxides.

Chemical analyses were carried out on the Cr, Mn, and Fe sorbents. As shown in Table XVI both the iron and manganese sorbents had sufficient metal oxide present to have a stoichiometric capacity of more than 10 percent SO_2.

The sorbents were exposed to standard flue gas as with the co-precipitated sorbents. In no case was the observed saturation capacity greater than 3 percent SO_2.

Figure 21

SORPTION/REGENERATION HISTORY OF SORBENT No. Ni-Al-1

Composition 26.4% NiO in Al_2O_3

Surface Area, m^2/gm 306

Stoichiometric Capacity, gm SO_2/100 gm sorbent 22.6

Sorbent Loading (gm SO_2/100 gm sorbent) vs. Time (arbitrary units)

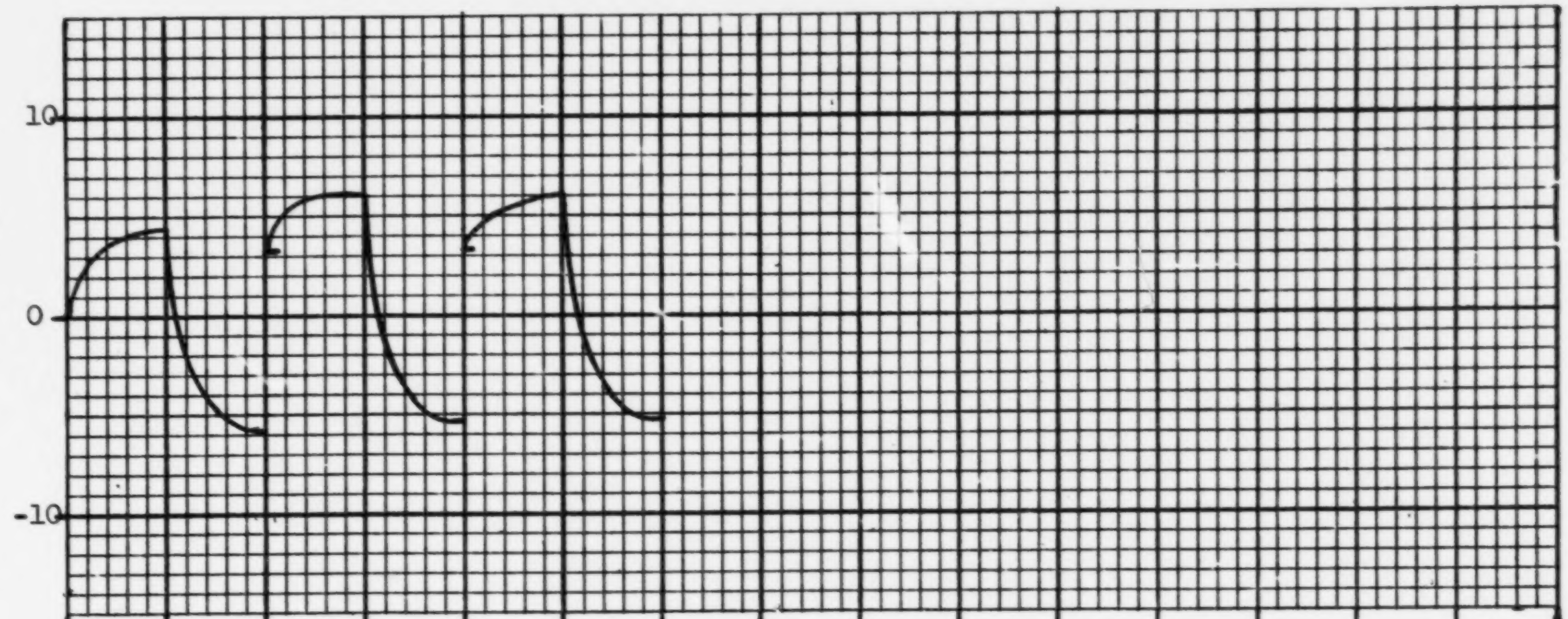

H_2 Regeneration	S1	R1	S2	R2	S3	R3									
Sorption/Regen. Temp., °C	300	650	450	650	550	650									
Initial Normalized Sorption Rate, % loading/% SO_2 hr.	189	-	221	-	106	-									
Ratio Measured/Stoichiom. Cap. %	19	-	11	-	12	-									
Sorption/Regeneration Half-time, min.	15	1	12	< 1	6	< 1									

Table XVI

Properties of Impregnated Sorbents

Material	Preparation Conditions					Composition (approx.)	Surface Area (m^2/gm)	X-Ray Diffraction Analysis
	Drying		Firing					
	Temp. (°C)	Time (hrs)	Temp. (°C)	Time (hrs)	Atm.			
I-0 Basic Alumina*	---			---		83% Al_2O_3 15% SiO_2	25.6	Quartz Al_2O_3
I-1 K_2O-Alumina*	---		650	7	H_2	---	6.8	Quartz, KNO_3 Al_2O_3
I-2 Na_2O-Alumina*	125	24	650	6	N_2	---	20.0	Quartz, $NaAl_{11}O_{17}$(wk) Al_2O_3, - Al_2O_3
I-3 NiO-Alumina*	125	24	650	6	N_2, H_2, Air	---	24.0	Quartz, NiO Al_2O_3
I-4 Cr_2O_3-Alumina*	125	(overnight)	650	10	N_2	2.4% Cr_2O_3	24.4	Quartz Al_2O_3
I-5 ZnO-Alumina*	125	(overnight)	650	14	H_2	---	22.8	---
I-6 CuO-Alumina*	125	(overnight)	650 600	11 (O.N.)	N_2 N_2	---	---	---
I-7 Mn_2O_3-Alumina*	125	(overnight)	650	13	H_2	7.3% Mn_2O_3	24.5	Quartz Al_2O_3
I-8 Fe_2O_3-Alumina*	125	(overnight)	650 650 600	10 4.5 5.0	N_2 N_2 N_2	9.2% Fe_2O_3	--- --- 22.4	Quartz Al_2O_3 Fe_3O_4 (weak)

* Norton Alumina - Catalyst Carrier No. LA-3032

Para-toluidene was also impregnated on alumina from a boiling ethanol solution. There was no sorption of SO_2 at 40°C, 60°C, or 100°C.

3. Commercially Available Sorbents

a. Florite (Floridin, Company, Pittsburgh, Pa.)

Florite is an activated bauxite containing largely alumina (75%) with some silica (15%) and Fe_2O_3 (3%). Samples of this material were exposed to flue gas. Saturation weight gains were on the order of 1-2%. Further study is not recommended.

b. Harshaw $CuO-Al_2O_3$ Catalyst

The catalyst was supplied with an analysis of 10% CuO by weight and a surface area of 137 m^2/gm. The sorbent was twice exposed to simulated flue gas at 450°C. The SO_2 concentration of the flue gas was nominally 0.25 percent by volume and the NO_x concentration 500 ppm. Sorbent loadings of over 6 gms SO_2/100 gms sorbent were obtained and saturation had not been reached. The stoichiometric saturation capacity is 13 grams SO_2/100 grams sorbent. Sorption rates were found to be much lower than with any of the other CuO-alumina sorbents.

c. Linde Mol-Sieve 5A

Saturation weight gains of 10.5 and 16 grams/100 grams of sorbent were obtained at 150°C and 100°C respectively, in a dry flue gas containing 1% SO_2. Saturation was complete after 40 minutes. A saturation weight gain of 9 grams/100 grams of sorbent was obtained in a dry flue gas containing 0.2% SO_2 at 100°C. Saturation required about 150 minutes. Regeneration was quickly accomplished in nitrogen at 350°C and activity was restored.

It is not known whether the sorption occurs as SO_2 or SO_3 so the weight gain may reflect SO_2 or SO_3 pickup. Capacities are reasonable but the rates are low. Also, it is not known whether water would preferentially occupy sites filled by SO_2 in these tests. CO_2 sorption at 100°C, however, was found to be only 1 gm/100 grams sorbent in 30 minutes from a gas containing 15% CO_2.

APPENDIX II

GLOSSARY

Term	Symbol	Meaning
Sorbent loading	w	Weight SO_2 sorbed/100 weights sorbent
Saturation loading	-	Final value of sorbent loading after exposure to flue gas for a sufficient period that weight gain has ceased.
Stoichiometric capacity	-	Sorbent loading stoichiometrically equivalent to conversion of all metal oxide to its normal sulfate.
Normalized sorption rate	$r(w)$	$r(w) = 1/y \ dw/dt$ where y = mole % SO_2 in gas t = time, hours
Average normalized sorption rate	$\bar{r}(w)$	$\bar{r}(w) = 1/y \ w/t$ where t = length of time sorption has occurred to achieve the loading w